LABORATORY DEMONSTRATION OF AIRCRAFT ESTIMATION USING LOW-COST SENSORS

by

John A. Sorensen
Control Technology Associates

NATIONAL AERONAUTICS AND SPACE ADMINISTRATION
Moffett Field, California

LABORATORY DEMONSTRATION OF AIRCRAFT STATE ESTIMATION USING LOW-COST SENSORS

John A. Sorensen
Control Technology Associates
Cupertino, CA 95014

SUMMARY

Four nonlinear state estimators were devised which provide techniques for obtaining the angular orientation (attitude) of the aircraft. These techniques are alternatives to direct measurement by use of vertical and directional gyros. These estimators have the potential of being of low cost and of high reliability by implementation using solid state instruments and the microcomputer.

An extensive FORTRAN computer program was developed to demonstrate and evaluate the estimators by using recorded flight test data. This program simulates the estimator operation, and it compares the state estimates with actual state measurements.

The above program was used to evaluate the state estimators with data recorded on the NASA Ames CV-990 and Cessna 402B aircraft From these evaluations, the preferred state estimator configuration was chosen. It was concluded that it is possible to estimate the aircraft attitude to the same degree of accuracy as is available by direct measurement.

A preliminary assessment was made of the memory, word length, and timing requirements for implementing the selected state estimator on a typical microcomputer.

CONTENTS

I

INTRODUCTION

Limited analytical studies have been made of using state estimation techniques coupled with low-cost sensors to replace the vertical and directional gyroscopes typically used on general aviation aircraft for flight control. These studies include previous work at Stanford University [1,2], an NRC Fellowship [3], and work at NASA Ames Research Center [4,5].

The objectives of this investigation were to

(1) Combine the previous efforts to define estimator configurations which: (a) have the best overall features of the previous work, and (b) provide the basis for further analysis, design, and flight testing.

(2) Specify the flight test data to be collected using the NASA Ames Cessna 402B aircraft. The data were to be used to test the estimator designs in the laboratory.

(3) Code the candidate estimator designs on the IBM 360 computer. Use the collected flight data to demonstrate the estimator performance under a variety of flight conditions and wind disturbances. Choose the estimator design yielding the best performance.

(4) Make recommendations regarding future system design and flight test efforts.

This report is organized as follows.

(1) Chapter II first presents details of previous estimator concepts which are suitable for determining the aircraft attitude without direct measurement. From these concepts, four nonlinear estimator configurations are designed. The method of implementing these equations digitally is explained.

(2) Chapter III presents results of evaluating the candidate estimators with both Convair CV-990 and Cessna 402B data. From this evaluation, the best estimator design is selected.

(3) Chapter IV presents preliminary requirements for implementing the selected estimator software on a typical microcomputer.

(4) Chapter V summarizes the work, lists distinct conclusions that have been made during the study, and makes recommendations for further research, testing, and development.

(5) Appendix A presents the details of the computer program developed for processing the flight data. It serves as a user's guide for additional flight data processing.

(6) Appendix B presents software details of the selected state estimator.

STATE ESTIMATOR SOFTWARE DESIGN

When investigating ways in which an aircraft's angular orientation could be determined without direct measurement, it rapidly became apparent that the estimator could be based on a wide choice of equation formulations. There have been several suggestions made [1-6] regarding how state estimators could be configured to obtain the aircraft attitude, and these are documented here. Then, composite methods which were chosen for implementation and testing with flight data are explained. Auxiliary software details are also presented.

The equations used to design the state estimators are based on well known aircraft equations of motion [7] and on a knowledge of the combinations of state variables measured by different instruments other than attitude gyros. The measurements that may be used include linear acceleration, angular acceleration, magnetic field, altitude, airspeed, and control surface deflection. Altitude and airspeed can be computed from measurements of static and dynamic pressure, while rate gyros may be substituted for angular accelerometers. The estimators basically combine rapid measurements of angular acceleration (or rate) with independent (although noisy) computations of the attitude angles (based on measurements of magnetic field data and other variables).

Previous Estimator Equations

Prior to beginning this effort, there were three alternate suggestions [2,3,5] for the configuration of the state estimator equations. These configurations were analyzed, and they served as the starting point for the composite estimation methods mechanized in this study. They are documented here for later reference.

Complementary filter approach [5]. Wingrove suggested a method which makes use of the following aircraft kinematic equations [7],

$$\ddot{h}_c = f_{xm} \sin \theta - f_{ym} \cos \theta \sin \varphi - f_{zm} \cos \varphi \cos \theta - g,$$

$$\dot{\varphi} = p + (q \sin \varphi + r \cos \varphi) \tan \theta,$$

$$\dot{\alpha} = q - p\beta + (g \cos \theta \cos \varphi + f_{zm})/V_{am},$$

3

$$\dot{\beta} = -r + p\alpha + (g \cos \theta \sin \varphi + f_{ym})/V_{am},$$

$$\dot{\psi}_{wind} = -f_{zm} \sin \varphi/V_{am} . \qquad (1)$$

These equations use the assumptions that α and β are small angles. In these and subsequent equations, the standard aircraft dynamics equation notation is used [7]. That is,

φ, θ, ψ - roll, pitch, yaw angles,

p, q, r - roll, pitch, yaw angular rates,

α, β - angles of attack and sideslip,

f_{xm}, f_{ym}, f_{zm} - body-fixed linear accelerometer readings,

V_{am} - measured true airspeed, and

ψ_{wind} - yaw (or heading) angle of velocity vector with respect to the airmass (wind).

Other equations used which transform from wind to body axes include:

$$\theta = \gamma_{wind} + \alpha \cos \varphi + \beta \sin \varphi,$$

$$\gamma_{wind} = \sin^{-1}(\dot{h}/V_{am}) ,$$

$$\psi_m = \psi_{wind} - \beta \cos \varphi + \alpha \sin \varphi. \qquad (2)$$

Here, additional notation used is:

γ_{wind} - flight path angle with respect to the airmass,

$\dot{h}$ - altitude rate,

ψ_m - yaw (or heading) angle of the longitudinal axis of the aircraft.

In addition, the aerodynamic equations which represent measured angle-of-attack (α_c) and sideslip (β_c) are

$$\alpha_c = \alpha_o + mf_{zm}/(C_{z\alpha}Q_mS) \ ,$$

$$= k_{\alpha 1} + k_{\alpha 2}\delta F_m + mf_{zm}/(C_{z\alpha}Q_mS) \ ,$$

$$\beta_c = mf_{ym}/(C_{y\beta}Q_mS) \ . \qquad\qquad (3)$$

Here, $k_{\alpha 1}$ and $k_{\alpha 2}$ are constants, δF_m is the flap angle, $C_{z\alpha}$ and $C_{y\beta}$ are aerodynamic coefficients, Q_m is the measured dynamic pressure, m is the aircraft mass, and S is the reference wing area. Use of Eqs. (3) assumes that stall conditions are not approached.

It is assumed that measurements of baro-altitude h_{baro}, true airspeed V_{am}, magnetic heading (or yaw) ψ_m, linear acceleration components (f_{xm}, f_{ym}, f_{zm}), angular acceleration components ($\dot{p}_m$, $\dot{q}_m$, $\dot{r}_m$), flap angle δF_m, and dynamic pressure Q_m are available. Then, Eqs. (1)-(3) are combined into the four coupled nonlinear, fixed-gain complementary filters [8] shown in Fig. 1. In this figure, the hats (^) on variables indicate that they are estimated. Also, the notations s and c are used to represent sine and cosine, respectively.

Note in Fig. 1 that an additional integrator is added to the front end of each channel. This is to remove the effect of possible biases which may exist in the linear and angular ¬celerometer measurements.

Vector approach [2]. DeBra suggested that the attitude angles could be determined by measurement of the gravity and magnetic field vectors g and B. The differential equations to obtain these smoothed vectors are

$$\dot{\hat{B}} = -\hat{\omega} \times \hat{B} + K_B(B_m - \hat{B}) \ ,$$

$$\dot{\hat{g}} = -\hat{\omega} \times \hat{g} + K_g(-f_m - \hat{g}) \ , \qquad\qquad (4)$$

where B_m is the three-component measurement from a three-axis magnetometer, and f_m is the measured vector from a three-axis linear accelerometer package. The vector $\hat{\omega}$ is the estimated attitude rate of the aircraft It could come from either integrating angular accelerometer outputs or direct (smoothed) rate gyro measurement. The quantities K_B and K_g are appropriate gain vectors.

$$h_c = -f_{zm}c\hat{\phi}c\hat{\theta} + f_{xm}s\hat{\theta} - f_{ym}c\hat{\theta}s\hat{\phi} - g \qquad n_4 = \hat{p}\hat{\alpha} + \hat{g}c\hat{\theta}s\hat{\phi} + f_{ym}$$

$$n_1 = (\hat{q}s\hat{\phi} + \hat{r}c\hat{\phi})\tan\hat{\theta} \qquad \hat{\dot{\theta}} = \sin^{-1}(\hat{\dot{h}}/V_{am}) + \hat{\alpha}c\hat{\phi} + \hat{\beta}s\hat{\phi}$$

$$n_2 = \hat{\beta}c\hat{\phi} - \hat{\alpha}s\hat{\phi} \qquad \hat{\psi} = \hat{\psi}_{wind} - \hat{\beta}c\hat{\phi} + \hat{\alpha}s\hat{\phi}$$

$$n_3 = -\hat{p}\hat{\beta} + (\hat{g}c\hat{\theta}c\hat{\phi} + f_{zm})/V_{am}$$
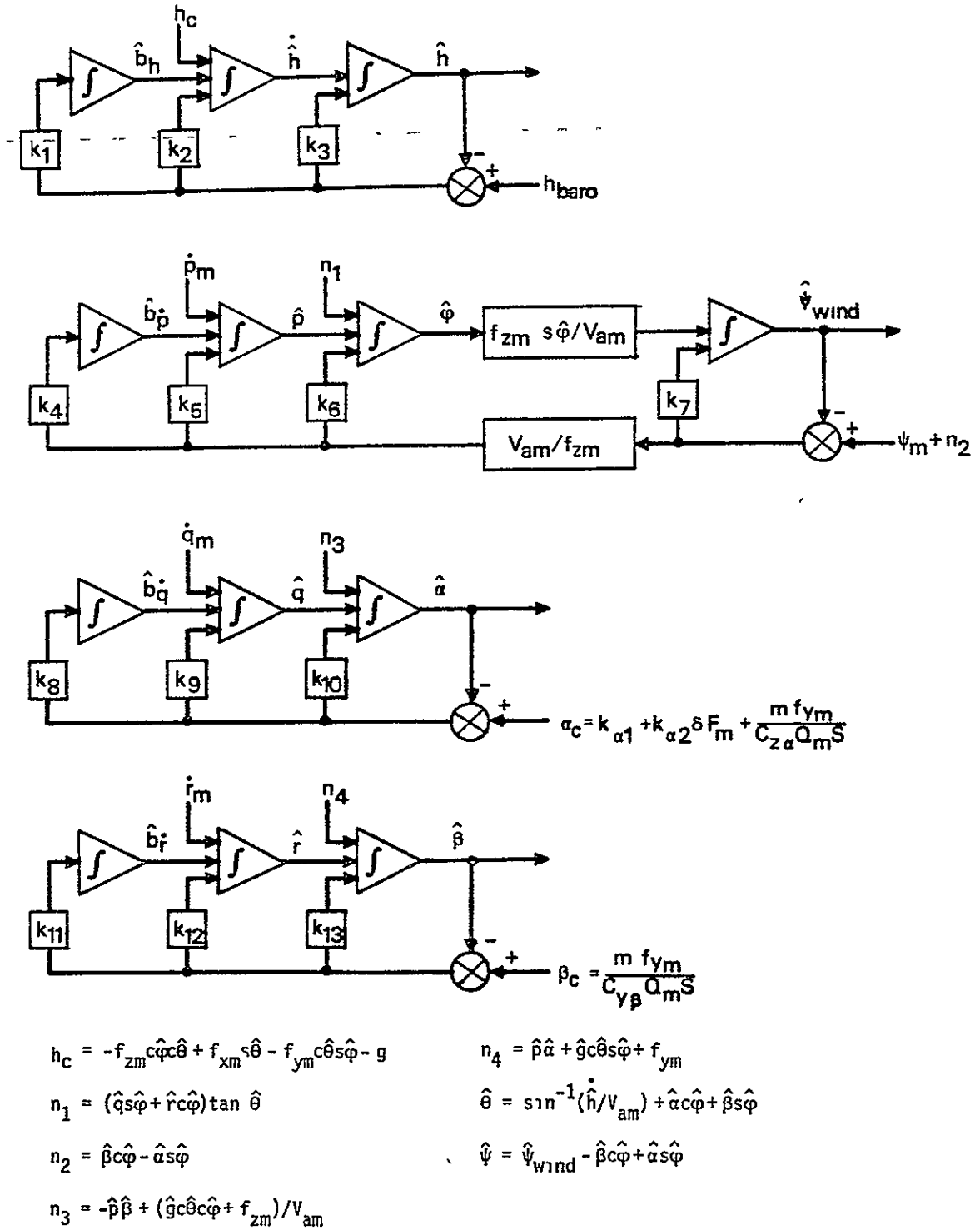
FIGURE 1.– COMPLEMENTARY FILTER FORM OF STATE ESTIMATOR [5]

With gravity and magnetic field vector estimates known, the direction cosine matrix which transfers from locally level to aircraft body axes is

$$C_{b/\ell} = \left[\frac{(\hat{g} \times \hat{B}) \times \hat{g}}{\left| g^2 B_{xo} \right|} \ \middle| \ \frac{\hat{g} \times \hat{B}}{\left| g B_{xo} \right|} \ \middle| \ \frac{\hat{g}}{\left| g \right|} \right]$$ (5)

Here, B_{xo} is the north component of B_m.

From this matrix, the roll, pitch, and yaw angles can be determined. Only the magnetic field dip angle has to be occasionally updated when using this method so that the north component of the field B_{xo} is kept current. The chief constraints of this method are that· (a) linear accelerometer readings are only valid (for their use in Eq. (4)) during unaccelerated flight, and (b) the accuracy of the attitude rate estimate $\hat{\omega}$ must allow adequate tracking of the gravity vector for prolonged maneuvers and periods of accelerated flight.

Kinematic filter approach [2,3]. Sorensen and Tashker devised linearized, decoupled longitudinal and lateral filters which were based on estimating the perturbations of the aircraft state variables from their nominal values. They were termed "kinematic filters" because they took advantage of the kinematic equations which represent the measurements of linear and angular accelerometers.

The matrix equation which represents the longitudinal kinematic filter is

$$
\begin{bmatrix} \Delta\hat{\dot{q}} \\ \Delta\hat{\dot{w}} \\ \Delta\hat{\dot{\theta}} \\ \Delta\hat{\dot{u}} \\ \Delta\hat{\dot{h}} \end{bmatrix}
=
\begin{bmatrix}
0 & 0 & 0 & 0 \\
U_o & 0 & -g\,s\,\theta_o & 0 \\
1 & 0 & 0 & 0 \\
-W_o & 0 & -g\,c\,\theta_o & 0 \\
0 & -c\,\theta_o & U_o\,c\,\theta_o + W_o\,s\,\theta_o & s\,\theta_o
\end{bmatrix}
\begin{bmatrix} \Delta q \\ \Delta w \\ \Delta\theta \\ \Delta u \\ \Delta h \end{bmatrix}
$$

$$
+
\begin{bmatrix} \Delta\dot{q}_m \\ \Delta f_{zm} \\ 0 \\ \Delta f_{xm} \\ 0 \end{bmatrix}
+
\begin{bmatrix} k_1 & 0 \\ 0 & k_2 \\ k_3 & 0 \\ k_4 & 0 \\ 0 & k_5 \end{bmatrix}
\begin{bmatrix} \Delta u_m - \Delta\hat{u} \\ \Delta h_m - \Delta\hat{h} \end{bmatrix}
\qquad (6)
$$

7

Here, the quantities U_o and W_o are the nominal values of longitudinal and normal airspeed. Also, θ_o is the nominal pitch angle.

The lateral kinematic filter is represented by

$$
\begin{bmatrix} \Delta\dot{\hat{p}} \\ \Delta\dot{\hat{r}} \\ \Delta\dot{\hat{\varphi}} \\ \Delta\dot{\hat{\psi}} \end{bmatrix} = \begin{bmatrix} 0 & 0 & 0 & 0 \\ 0 & 0 & 0 & 0 \\ 1 & \tan\theta_o & 0 & 0 \\ 0 & \sec\theta_o & 0 & 0 \end{bmatrix} \begin{bmatrix} \Delta\hat{p} \\ \Delta\hat{r} \\ \Delta\hat{\varphi} \\ \Delta\hat{\psi} \end{bmatrix} + \begin{bmatrix} \Delta\dot{p}_m \\ \Delta\dot{r}_m \\ 0 \\ 0 \end{bmatrix}
$$

$$
+ \begin{bmatrix} k_6 & 0 \\ 0 & k_7 \\ k_8 & 0 \\ 0 & k_9 \end{bmatrix} \begin{bmatrix} \Delta\varphi_m - \Delta\hat{\varphi} \\ \Delta\psi_m - \Delta\hat{\psi} \end{bmatrix}. \tag{7}
$$

In Eqs. (6) and (7), the "Δ" notation represents perturbations from the nominal. The subscript "m" on input variables ($\dot{p}_m$, $\dot{q}_m$, $\dot{r}_m$, f_{xm}, f_{zm}, u_m, h_m, φ_m, ψ_m) indicates that these variables are independently measured or computed.

These equations must be expanded to include cross coupling terms, and they do not have to be restricted to small perturbations. Also, it was recognized that if an independent measurement of pitch angle θ_m were available, this could be used to replace the residual in airspeed ($u_m - \hat{u}$) for the longitudinal equations. Thus, the resulting nonlinear kinematic filter is represented by the schematic diagrams in Fig. 2. In this representation, it is assumed that the pitch angle $\hat{\theta}$ remains small.

Note that the kinematic filter in Fig. 2 has the same complementary form as the filter suggested by Wingrove in Fig. 1 Also, note that the altitude $\hat{h}$ channel uses the longitudinal component of airspeed U as a separate input.
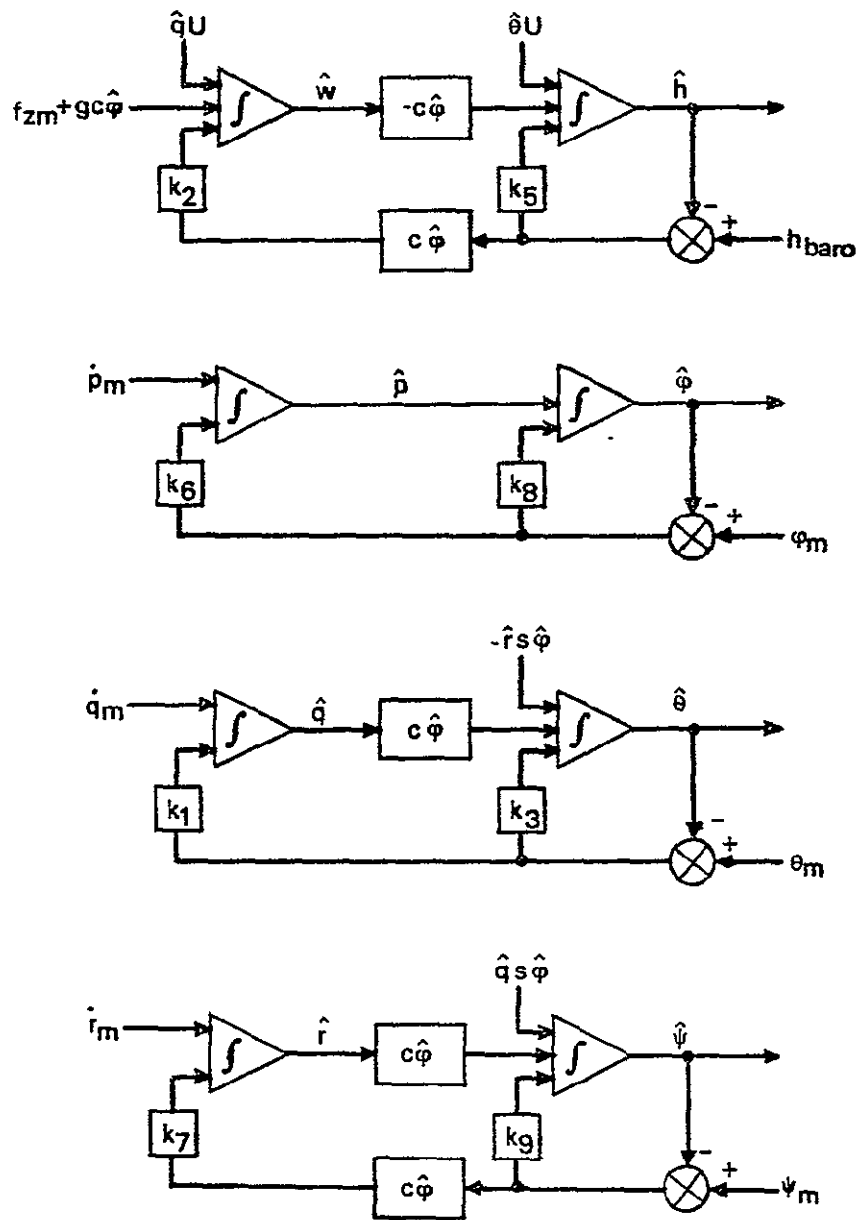
8

FIGURE 2.- COUPLED NONLINEAR KINEMATIC FILTER FORM
OF STATE ESTIMATOR [2,3]

9

Development of Composite Nonlinear Estimators

For flight test investigation of the estimator concept, it is desirable to reduce the number of forms of estimators to one which has the best overall features. This is not possible without laboratory testing several configurations with actual data, this provided the motivation for this study.

In examining the estimator concepts just discussed, some important points were developed:

(1) It seemed advisable to retain the complementary filter form found in Figs. 1 and 2. This would enable combining the fast response angular accelerometer data (which would tend to drift) with stable, although noisy, independent measurements of the three attitude angles.

(2) Because roll and heading angles could both be determined from magnetometer data, it seemed reasonable to have separate channels for these quantities (as in Fig. 2 rather than Fig. 1).

(3) To simplify the estimator, the sideslip angle β (as in Fig. 1) was assumed to be zero. This feature could be added later, if required.

(4) Two methods existed for computing independent measurements of the attitude angles (φ_m, θ_m, ψ_m)--the vector approach discussed on page 5, and a method which computes roll and heading given pitch, which is discussed later. It was not clear which of these methods was preferable. Thus, two forms of the composite estimators were first posed.

As the study proceeded, two additional forms of the state estimators developed. These four methods are now explained.

Method 1. The basic form of the nonlinear estimator used in method 1 is shown in Fig. 3. This assumes inputs ($\dot{p}_m$, $\dot{q}_m$, $\dot{r}_m$) from three body-fixed orthogonal, angular accelerometers. The three attitude estimates are ($\hat{\varphi}$, $\hat{\theta}$, $\hat{\psi}$). The three independent computations of roll, pitch, and heading are denoted as (φ_c, θ_c, ψ_c).

The form of Fig. 3 was derived by combining and extending the design of Figs. 1 and 2. Note that if rate measurements (p_m, q_m, r_m) were directly available, only three integrations, rather than six, would be required to implement this form. The
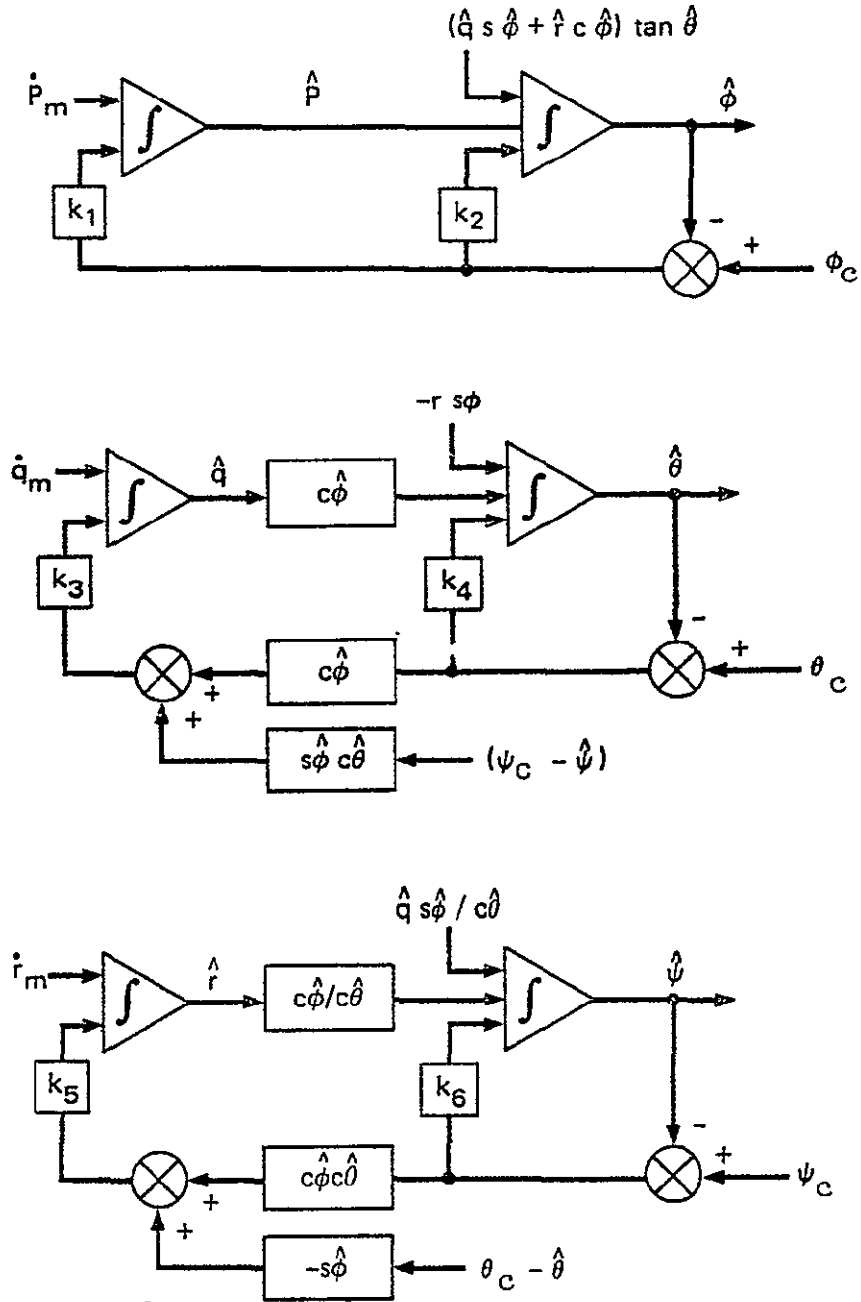
FIGURE 3.- BASIC FORM OF THE NONLINEAR ESTIMATOR
TO COMPUTE (φ, θ, ψ)

11

decision of whether to use rate measurement devices or angular accelerometers must be based on reliability and cost considerations which were not a part of this study.

Note in Fig. 3 that the nonlinear terms in the feed-forward paths of each channel come from the dynamic equations which relate the aircraft body rates (p, q, r) to the Euler angle rates ($\dot{\phi}$, $\dot{\theta}$, $\dot{\psi}$) [7]. The nonlinear terms in the feedback paths for the pitch (θ) and heading (ψ) channels relate the orientation of these Euler axes to the body axes representing pitch rate (q) and yaw rate (r).

If the angular accelerometer measurements are subject to bias, the bias effects are removed (since they are observable) by expanding each complementary filter to third order, as is illustrated in Fig. 4 for the roll channel.

To compute altitude rate $\dot{\hat{h}}$, and an estimate of flight path angle $\hat{\gamma}$, a fourth complementary filter is added. This is depicted in Fig. 5, and it is the same as the altitude

FIGURE 4.- MODIFICATION OF ROLL ESTIMATOR TO COMPENSATE
FOR ANGULAR ACCELEROMETER BIAS

FIGURE 5.- COMPLEMENTARY FILTER TO OBTAIN
SMOOTHED ALTITUDE

12

channel in Fig 1. This filter complements barometric altitude h_{baro} with a computation of vertical acceleration $\dot{h}_c$ which is given in Eqs. (1). The estimated flight path angle and angle-of-attack are then computed as

$$\hat{\gamma} = \sin^{-1}(\dot{\hat{h}}/V_{am}) \quad ,$$
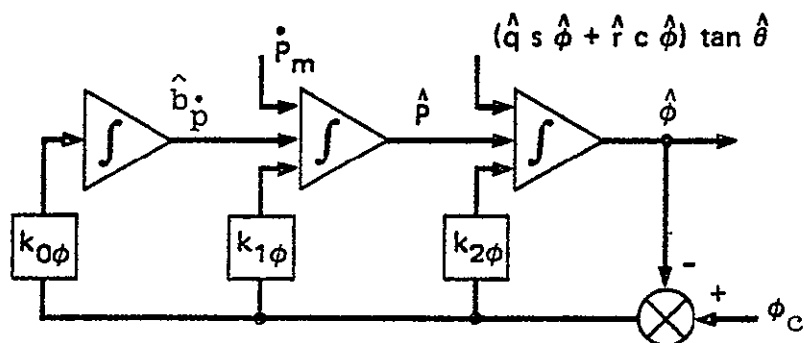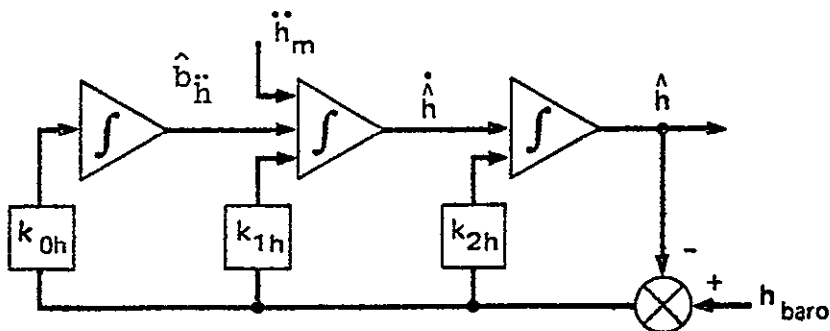
$$\hat{\alpha} = (\hat{\theta} - \hat{\gamma})/\cos \hat{\varphi} \quad , \tag{8}$$

where V_{am} is the measured airspeed.

In this method, the vector approach, discussed earlier, is used to compute independent measurements of $(\varphi_c, \theta_c, \psi_c)$. The earth's magnetic field measurements are used directly. Estimates of the earth's gravity vector are obtained from the second of Eqs. (5). For this approach to work, digital logic must be used to cut out the accelerometer inputs to this equation when it is sensed that the aircraft is turning or accelerating

Assume that the aircraft rotates, in order, through Euler angles (ψ, θ, φ) from the north-oriented locally-level reference frame to the aircraft fixed body frame. If c_{ij} (with $i,j = 1,2,3$) are components of $C_{b/\ell}$ given by Eq. (5), then one can compute

$$\sin \theta_c = - c_{13} \quad ,$$

$$\sin \varphi_c = c_{23}/\cos \theta_c \quad ,$$

$$\sin \psi_c = c_{12}/\cos \theta_c \quad ,$$

$$\cos \psi_c = c_{11}/\cos \theta_c \quad . \tag{9}$$

Equations (9) are then solved for the independent measurements of $(\varphi_c, \theta_c, \psi_c)$.

Method 2. In this method, the second channel in Fig. 3 is changed to estimate angle-of-attack $\hat{\alpha}$ rather than pitch angle $\hat{\theta}$. The channel is replaced by the one shown in Fig 6, which also compensates for the pitch accelerometer bias. This is essentially the same as the third channel of the complementary filter depicted in Fig. 1.

The complementary measurement of the angle-of-attack comes from the first of Eqs. (3). In this method, flap angle δF_m and dynamic pressure Q_m measurements are required as well as knowledge of aircraft characteristics m, S, C_{Z_α}, and α_o as a function of flap angle.

13
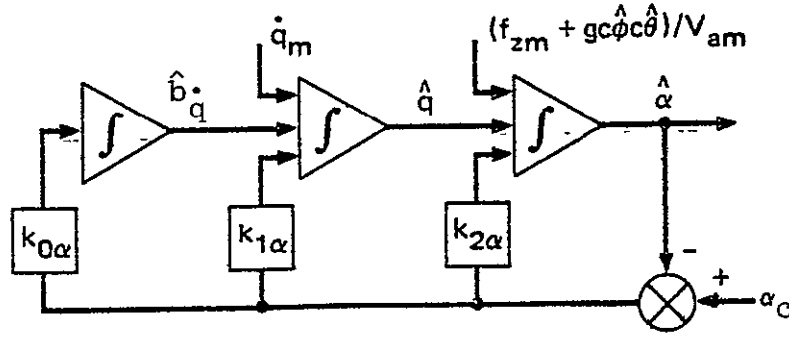
FIGURE 6.— MODIFICATION OF FILTER TO COMPUTE
ANGLE-OF-ATTACK

From the smoothed angle-of-attack, the estimated pitch angle is computed to be

$$\theta_c = \hat{\alpha} \cos \hat{\varphi} + \sin^{-1}(\dot{\hat{h}}/V_{am}) \tag{10}$$

With the pitch angle θ_c determined, the roll and heading angles φ_c and ψ_c can be computed directly from the magnetic field measurements B_m. This has the advantage that the gravity vector estimate $\hat{g}$ is not required, as in Method 1.

The relationship between the aircraft-fixed components of B_m and the North-oriented, locally-level reference components (B_{x_O}, O, B_{z_O}) are

$$
\begin{bmatrix} B_{x_m} \\ B_{y_m} \\ B_{z_m} \end{bmatrix} =
\begin{bmatrix}
c\theta c\psi & c\theta s\psi & -s\theta \\
s\varphi s\theta c\psi - c\varphi s\psi & s\varphi s\theta s\psi + c\varphi c\psi & s\varphi c\theta \\
c\varphi s\theta c\psi + s\varphi s\psi & c\varphi s\theta s\psi - s\varphi c\psi & c\varphi c\theta
\end{bmatrix}
\begin{bmatrix} B_{x_O} \\ O \\ B_{z_O} \end{bmatrix} \tag{11}
$$

Here, the notations s and c are used to represent sine and cosine, respectively.

From Eqs. (11), the cosine of the heading angle is found to be

$$\cos \psi_c = (B_{x_m} + B_{z_O} \sin \theta_c)/B_{x_O} \cos \theta_c . \tag{12}$$

14

Here, it is assumed that the local values of B_{x_O} and B_{z_O} are known and stored, or are computed by other means, as is discussed later.

Also from Eq. (11), a quadratic expression can be found for the cosine of the roll angle

$$[(B_{z_m}^2 + B_{y_m}^2)c^2\theta_c]c^2\varphi_c - 2[(B_{z_O} + B_{x_m} s\theta_c)B_{z_m}c\theta_c]c\varphi_c$$

$$+ [(B_{z_O} + B_{x_m}s\theta_c)^2 - B_{y_m}^2 c^2\theta_c] = 0 \ . \qquad (13)$$

With the two solutions $(\cos \varphi_{c_1}, \cos \varphi_{c_2})$ for Eq. (13), the following expression is used to solve for two corresponding solutions of the sine of the roll angle

$$\sin \varphi_{c_1} = B_{y_m}(c^2\varphi_{c_1}-1)/(B_{z_m}c\varphi_{c_1} - B_{z_O}c\theta_c - B_{x_O}s\theta_c c\psi_c),$$

$$\imath = 1,2 \qquad (14)$$

Then

$$\tan \varphi_{c_i} = \sin \varphi_{c_i}/\cos \varphi_{c_1} \ , \qquad i=1,2 \ . \qquad (15)$$

Two ways are used to resolve the ambiguity in the solution for φ_c. In one case, a trial value φ_t is computed that is based on the previously computed values, φ_{c-1}.

$$\varphi_t = \varphi_{c-1} + \hat{p} \ \Delta t \ . \qquad (16)$$

Here, $\hat{p}$ is the estimate of the roll rate, and Δt is the sample period. Then, the solution to Eq. (15) is picked which is closer to Eq. (16).

The other way to resolve the ambiguity is to assume that the aircraft usually makes coordinated turns. Then, the trial solution of roll angle is found from the coordinated turn relationship,

$$\tan \varphi_t = V_a \dot{\psi}/g \ ,$$

$$= V_{am} (\hat{q} \sin \hat{\varphi} + \hat{r} \cos \hat{\varphi})/g \cos \theta_c \ . \qquad (17)$$

Here, V_{am} is the measured airspeed, and $\hat{q}$, $\hat{r}$, and $\hat{\varphi}$ are estimated values of pitch rate, yaw rate, and roll angle obtained from the estimator. Again, with this trial solution, the closer value of Eq. (15) is selected.

Finally, the equation

$$\sin \psi_c = (s\varphi_c - B_{y_m}c\varphi_c/B_{z_m})(B_{z_m}/B_{x_o}) \qquad (18)$$

is used to solve for ψ_c.

A potential problem exists with this method in that the solutions to Eq. (13) converge as ψ gets close to $0°$ or $180°$. This is partially solved by use of Eqs. (16) or (17). However, Eq. (17) contains $\hat{\varphi}$ which could also be in error. Also, noise in $\hat{p}$ or φ_{c-1} in Eq. (16) could cause the wrong value to be selected.

Method 3. Although the techniques used to resolve the ambiguity problem for Method 2 worked for the data examined in this study, it was felt that certain data inputs could still produce incorrect solutions to the computed roll and heading Eqs. (12)-(18). Thus, for Method 3, Eq. (17) was used directly to compute φ_c. Equation (10) was still used to compute θ_c. Then, Eqs. (12) and (18) were used to compute ψ_c.

One shortcoming of this method is that it relies on the coordinated turn assumption. The information contained in the magnetic data is not fully used. Also, as can be seen from Eq. (17), the computed roll angle φ_c is not independent of the estimate $\hat{\varphi}$. Flight tests under sideslip conditions are required to determine if this seriously degrades the performance of the estimator.

Method 4. Recall that the prime motivation for this research is to provide a low-cost alternative to direct measurement of the aircraft attitude angles. Thus, it is desirable to keep the estimators as simple as possible.

The estimators developed in the previous three methods use a three-axis angular accelerometer package (or alternately, three rate gyros) to provide fast response attitude change measurements. But it is well known to pilots [9] that altitude, airspeed, yaw rate, and lateral acceleration measurements provide adequate information to fly straight-and-level. To these, heading angle measurements (from a compass) allow keeping a correct course. Thus, there was reason to believe

16

that a simpler configuration than that of the previously described three methods could be developed.

A method, suggested by Denery [6], makes use of a single yaw rate gyro measurement r_m. The equation for lateral acceleration is

$$\dot{V} + rU - pW = a_y + g \cos \theta \sin \varphi . \tag{19}$$

Here, a_y is the lateral acceleration due to aerodynamics, and (U,V,W) are body-fixed components of V_a. If $\dot{V}$ and pW are assumed to be negligible, Eq. (19) can be rewritten as

$$\sin \varphi_c = (r_m V_{am} \cos \alpha_c - f_{y_m})/g \cos \theta_c , \tag{20}$$

where f_{y_m} is the measured lateral acceleration and V_{am} is the measured total airspeed V_a. The pitch angle θ_c again comes from Eq. (10). The angle-of-attack α_c is from Eqs. (3). Equation (2) is solved for roll angle φ_c.

The equation for normal acceleration is

$$\dot{W} + pV - qU = a_z + g \cos \theta \cos \varphi . \tag{21}$$

If $\dot{W}$ and pV are assumed to be negligible, Eq. (21) has the following solution for pitch rate:

$$q_c = -(f_{z_m} + g \cos \theta_c \cos \varphi_c)/V_{am} \cos \alpha_c . \tag{22}$$

Here, φ_c comes from Eq. (20). Then, the heading rate $\dot{\psi}_c$ is computed to be

$$\dot{\psi}_c = (q_c \sin \varphi_c + r_m \cos \varphi_c)/\cos \theta_c . \tag{23}$$

This equation is smoothed using the first-order complementary filter

$$\dot{\hat{\psi}} = \dot{\psi}_c + k_\psi(\psi_m - \hat{\psi}) , \tag{24}$$

where ψ_m comes from the magnetic field measurements and Eqs. (12) and (18).

17

In this method, most of the complementary filter structure is removed. Only four integrators (three to compute $\dot{h}$ as in Fig. 5 and one for Eq. (24)) are required instead of twelve. The shortcomings of Method 4 are the assumptions used to obtain Eqs. (20) and (22).

Digitization and Auxiliary Software

To mechanize the state estimators in digital form for flight testing, some additional software was required. Also, modifications of the continuous filter differential equations described previously to discrete form were required. These additions and modifications are explained here.

<u>Instrumentation corrections and computations</u>.- Corrections and modifications must be made to the sampled signals used as inputs to the state estimators to remove known error effects. The linear accelerometers are subject to misalignment with respect to the aircraft reference body axis. Center-of-gravity (c.g.) offsets are also present which may require compensation. If $(f_{x_m}, f_{y_m}, f_{z_m})$ are the sampled accelerometer readings, and $(\varphi_{a_m}, \theta_{a_m}, \psi_{a_m})$ represent the small misalignment angles, then the corrected readings are

$$
\begin{bmatrix} f'_{x_m} \\ f'_{y_m} \\ f'_{z_m} \end{bmatrix} = \begin{bmatrix} 1 & \psi_{a_m} & -\theta_{a_m} \\ -\psi_{a_m} & 1 & \varphi_{a_m} \\ \theta_{a_m} & -\varphi_{a_m} & 1 \end{bmatrix} \begin{bmatrix} f_{x_m} \\ f_{y_m} \\ f_{z_m} \end{bmatrix} . \tag{25}
$$

Also, if $(x_{a_m}, y_{a_m}, z_{a_m})$ are the position coordinates of the accelerometer package with respect to the average aircraft c.g., then these accelerometer readings are further modified to

$$
f''_{x_m} = f'_{x_m} - \dot{q}_m z_{a_m} + \dot{r}_m y_{a_m} + (\hat{q}^2 + \hat{r}^2)x_{a_m} - \hat{p}(\hat{q}y_{a_m} + \hat{r}z_{a_m}) ,
$$

$$
f''_{y_m} = f'_{y_m} - \dot{r}_m x_{a_m} + \dot{p}_m z_{a_m} + (\hat{p}^2 + \hat{r}^2)y_{a_m} - \hat{q}(\hat{p}x_{a_m} + \hat{r}z_{a_m}) ,
$$

$$
f''_{z_m} = f'_{z_m} - \dot{p}_m y_{a_m} + \dot{q}_m x_{a_m} + (\hat{p}^2 + \hat{q}^2)z_{a_m} - \hat{r}(px_{a_m} + \hat{q}y_{a_m}) .
$$

$$\tag{26}$$

18

In Eq. (26), the acceleration terms $(\dot{p}_m, \dot{q}_m, \dot{r}_m)$ come from the angular accelerometers, the rate terms $(\hat{p}, \hat{q}, \hat{r})$ come from the estimator.

In addition, the accelerometers are subject to biases $(b_{axc}, b_{ayc}, b_{azc})$ and scale factor errors $(\varepsilon_{axc}, \varepsilon_{ayc}, \varepsilon_{azc})$. If these terms are known, the readings are further corrected by the equations

$$f_{xm} = (1 + \varepsilon_{axc})f_{xm}'' + b_{axc} ,$$

$$f_{ym} = (1 + \varepsilon_{ayc})f_{ym}'' + b_{ayc} ,$$

$$f_{zm} = (1 + \varepsilon_{azc})f_{zm}'' + b_{azc} . \tag{27}$$

The angular accelerometer and magnetometer are also subject to misalignments, biases, and scale factor errors. If these errors are known, the sampled readings are also corrected by equations similar to Eqs. (25) and (27).

If airspeed is derived from a pitot tube, the reading represents a component along the pitot tube axes. This reading V_m must first be converted from indicated airspeed to true airspeed V_m', by the equation

$$V_m' = V_m \sqrt{\rho_0/\rho} = V_m/\sqrt{\sigma} . \tag{28}$$

Here, σ is the density ratio which is a function of altitude. Computation of σ is done from a table as a function of altitude by interpolation. Such a procedure is explained in Appendix A.

The airspeed measurement is then filtered by the equation

$$\hat{U}_{n+1} = \hat{U}_n + k_u\Delta t(V_m' - \hat{U}_n) . \tag{29}$$

Here,

k_u = airspeed filter gain,

$\hat{U}_n$ = smoothed value of V_m , and

Δt = sample period.

19

The subscripts n and n+1 indicated current and predicted values (one sample period later). Then, if θ_v is the rotation of the pitot tube up from the aircraft longitudinal axis, the components of the aircraft velocity are

$$\hat{U} = (-\hat{U}_n \cos \hat{\theta} + \dot{\hat{h}} \sin \bar{\theta}_v)/(\sin \theta_v \sin \hat{\theta} - \cos \theta_v \cos \hat{\theta}),$$

$$\hat{W} = (-\hat{U}_n \sin \hat{\theta} + \dot{\hat{h}} \cos \theta_v)/(\sin \theta_v \sin \hat{\theta} - \cos \theta_v \cos \hat{\theta}),$$

$$\hat{V}_{am} = \hat{U} \cos \hat{\alpha} + \hat{W} \sin \hat{\alpha} . \tag{30}$$

In Eqs. (30), the terms $\hat{\theta}$, $\dot{\hat{h}}$, and $\hat{\alpha}$ come from the estimator.

If the J-Tek Airspeed Sensor is used, total true airspeed V_{am} is sensed directly. Then, this is smoothed by the equation

$$\hat{V}_{am_{n+1}} = \hat{V}_{am_n} + k_u \Delta t (V_{am} - \hat{V}_{am_n}) . \tag{31}$$

If dynamic pressure Q is not measured, it can be derived from the true airspeed by the equation

$$\hat{Q}_n = 0.5 \, \rho \hat{V}_{am}^2 = 0.001189 \, \sigma \hat{V}_{am}^2 . \tag{32}$$

Again, the density ratio σ is computed as a function of altitude $\hat{h}$.

One further computation is required to determine the magnetic vector dip angle δ_2. This is used to compute the north and down components B_{xo} and B_{zo} found in Eqs. (11). If the magnetic field has unity magnitude, then these components have the values

$$B_{xo} = \cos \delta_2 ,$$

$$B_{zo} = \sin \delta_2 \tag{33}$$

For a typical flight, the dip angle will be slowly varying as a function of aircraft geographical position. Thus, the dot product between the magnetic field vector B and the gravity

20

vector g would also vary slowly. This fact can be used to update δ_2 by the equation

$$\delta_{2n+1} = \delta_{2n} + k_\delta \left[\sin^{-1} \left(\frac{B_m \cdot f_m}{|B_m| |f_m|} \right) - \delta_{2n} \right] \Delta t \tag{34}$$

Here, k_δ is a slow gain, and B_m and f_m are magnetometer and linear accelerometer measurements of B and g.

Digitization.- Note that the nonlinear estimators depicted in Figs. 1-6 are in continuous (analog) form. To mechanize these filter equations on a digital computer required making some assumptions about the nature of the cross-coupling terms and feedback quantities. The assumptions for the roll estimator shown in Fig. 4 were:

(1)   The sample period is very small.

(2)   All trigonometric functions ($\sin \varphi$, $\cos \varphi$, $\tan \theta$) are constant over the sample period.

(3)   The feedback correction term ($\varphi_c - \hat{\varphi}$) is constant over the sample period.

The same type of assumptions were made for the altitude, yaw, and pitch (or angle-of-attack) filters.

With these assumptions, the following expressions represent examples of the discrete update equations used for the roll estimator:

Roll accelerometer bias, $\hat{b}_{\dot{p}}$

$$r_\varphi = \varphi_{c_n} - \hat{\varphi}_n \ ,$$

$$c_{b_p} = k_{o\varphi} \, r_\varphi \ ,$$

$$\hat{b}_{\dot{p}_{n+1}} = \hat{b}_{\dot{p}_n} + c_{b_p} \, \Delta t \ . \tag{35}$$

Roll rate, $\hat{p}$

$$c_3 = \dot{p}_{m_n} + k_{1\varphi} \, r_\varphi + \hat{b}_{\dot{p}_n} \ ,$$

$$\hat{p}_{n+1} = \hat{p}_n + c_3 \, \Delta t + c_{b_p} \, \Delta t^2/2 \ . \tag{36}$$

21

Roll angle, $\hat{\varphi}$

$$c_4 = k_{2\varphi} \, r_\varphi \; ,$$

$$\hat{\varphi}_{n+1} = \hat{\varphi}_n + [\hat{p}_n + (\hat{q}_n \sin \hat{\varphi}_n + \hat{r}_n \cos \hat{\varphi}_n) \tan \hat{\theta}_n + c_4] \Delta t$$

$$+ [c_3 + (c_5 \sin \hat{\varphi}_n + c_7 \cos \hat{\varphi}_n) \tan \hat{\theta}_n] \Delta t^2 / 2$$

$$+ [c_{b_p} + (c_{b_q} \sin \hat{\varphi}_n + c_{b_r} \cos \hat{\varphi}_n) \tan \hat{\theta}_n] \Delta t^3 / 6.$$

$$(37)$$

In Eqs. (35)-(37), the subscript $n+1$ again indicates the updated value projected one sample period Δt into the future. The subscript n represents the current estimated values. Also, in Eq. (37), the quantities c_5 and c_7 represent terms similar to c_3 (Eq. (36)) from the pitch and roll channels, respectively. The terms c_{b_q} and c_{b_r} represent terms similar to c_{b_p} (Eq. (35)), also from the pitch and roll channels. Further details of these expressions and for the other channels are found in Appendices A and B.

With fast sampling rates (five or more samples per second), the direct integration implied by the Eqs. (35)-(37) produces adequate accuracy. If the sample rate were to decrease, modifications would be necessary to account for these effects. Such methods for implementation of sampled data systems such as Tustin's method and the hold equivalence [10] have been developed to provide discrete transfer functions with the same characteristics as the continuous system. Investigation of these procedures was beyond the scope of this effort.

Gain selection.- The gains for the filters shown in Fig. 3 are found by assuming that the coupling terms between the roll, pitch, and heading equations are zero, this decouples them into three linear second-order filters. They have characteristic equations

$$s^2 + 2\zeta \, \omega_n s + \omega_n^2 = 0 \; . \tag{38}$$

For these filters, the error characteristics of the accelerometer inputs ($\dot{p}_m$, $\dot{q}_m$, $\dot{r}_m$) and the angles computed from magnetometer data (φ_m, θ_m, ψ_m) were unknown. To obtain some

22

appropriate gains with which to begin to test the estimators with flight data, it was assumed that the input errors could be modeled as white noise with Gaussian distribution. Then, Kalman filter theory [11] was used to compute the gains.

With this assumption, the gains for the roll filter of Fig. 3, for example, are

$$k_1 = \omega_n^2 = \sigma_{\dot{p}}/\sigma_{\varphi_m} \quad ,$$

$$k_2 = 2\zeta \, \omega_n = 1.414 \, \sqrt{k_1} \quad . \tag{39}$$

Here, $\sigma_{\dot{p}}$ is the assumed standard deviation of the roll accelerometer measurement noise. Also, σ_{φ_m} is the assumed standard deviation of the independent roll angle computation noise. Similar methods are used to compute gains $k_3 - k_6$.

If bias terms are added to the estimator (such as in Fig. 4), the filter equations are observable but not disturbable [12]. Thus, the Kalman filter theory cannot be used directly. To make this adjustment, the filters' characteristic equations were expanded to the assumed form

$$(s^2 + 2\zeta \, \omega_n s + \omega_n^2)(s + \omega_n) = 0 \quad . \tag{40}$$

Then, the resulting gains become

$$k_o = \omega_n^3 \quad ,$$

$$k_1 = (1 + 2\zeta) \, \omega_n^2 \quad ,$$

$$k_2 = (1 + 2\zeta) \, \omega_n \quad . \tag{41}$$

Again, ω_n^2 was taken to be $\sigma_{\dot{p}}/\sigma_{\varphi_m}$, and the damping term ζ was $\sqrt{2}/2$. Similar methods were used for gain selection in the pitch (or angle-of-attack), yaw, and altitude filters.

STATE ESTIMATOR PERFORMANCE EVALUATION

After developing the candidate state estimator configurations, the next step was to analyze them using recorded flight test data. The purposes of this step were to:

(1) Demonstrate that the estimators actually worked as predicted using real (rather than simulated) input data. This is a step closer to actual flight test.

(2) Compare the performance of the estimation methods so that a final configuration could be chosen.

(3) Note the limitations of the estimators in severe wind conditions, unusual aircraft attitudes, and the presence of typical instrument errors.

The details of the evaluation are now discussed.

Evaluation Procedure

To enable evaluating the estimator methods, a FORTRAN digital computer program was developed for the NASA Ames IBM 360/67 which simulated operation of the digital estimator methods described in Chapter II. A complete description of this program, its inputs, its output, and its various capabilities are documented in the form of a user's guide in Appendix A.

The program is set up to read in sequentially recorded, sampled, digital flight data. These data act as the driver for the program. The program makes necessary pre-estimation computations and then simulates the operation of the digital software as it operates in a sequential fashion. After the data are read in, the steps executed are·

(1) All sensor data not actually present are artificially generated. For example, rate gyro data are smoothed and then differentiated to produce artificial angular accelerometer data.

(2) Artificial errors are optionally added to the data to allow determining the resulting effect on estimate accuracies. By varying the error magnitudes, the program user can obtain performance sensitivity data These sensitivity data are useful for specifying sensor accuracy requirements.

25

(3)   The data are filtered and modified with correction terms to remove known sensor errors. For example, obvious biases are removed from the linear accelerometer readings. This is the first step in the simulated estimator software.

(4)   The independent calculations of roll, pitch, and heading (φ_c, θ_c, ψ_c) angles are made. An option flag determines which computation method described in Chapter II is used.

(5)   The primary filter equations are executed to produce estimates of attitude angles and rates ($\hat{\varphi}$, $\hat{\theta}$, $\hat{\psi}$, $\hat{p}$, $\hat{q}$, $\hat{r}$), angle-of-attack $\hat{\alpha}$, and flight path angle $\hat{\gamma}$. Also, smoothed values of altitude $\hat{h}$ and true airspeed $\hat{V}_a$ are generated.

(6)   The results are compared to directly-measured values of the state variables. For example, the estimated attitude angles are compared to angles measured by an LTN-51 inertial navigation system. Comparison consists of computing the means and standard deviations between the estimated (or smoothed) and directly measured data.

(7)   The results are recorded either in numerical or plot form.

When the program coding and debugging was completed, anticipated data from the Cessna 402 aircraft were not yet available. Therefore, data from a Convair CV-990 flight were used to check out the program. These data did not contain magnetometer measurements, so these quantities were artificially generated from the INS measurements.

The CV-990 data were divided into three segments that tested the estimator configurations under longitudinal motion, lateral motion, and both modes together. Details of these data are described later.

The four estimator methods described in Chapter II were each tested with the three segments of CV-990 data. From these runs, it was shown that each of the methods works to varying degrees of accuracy with actual data. Thus, it was further concluded that the concept of estimating attitude angles, rather than direct measurement, is valid.

Towards the end of this study, a small amount of data (80 sec) taken from the Cessna 402 aircraft became available. This provided additional information because the data included actual magnetometer measurements. The estimators were tested with this data, and further conclusions were made.

Test results from using the CV-990 and C-402 data are now discussed.

CV-990 Performance Results

The Ames CV-990 instrumentation and associated measurements included:

Inertial navigation system	$-$ φ, θ (ψ not available)
Directional gyro	$-$ ψ
Three-axis linear accelerometer	$-$ f_x, f_y, f_z
Three-axis rate gyros	$-$ p, q, r
Baro-altimeter	$-$ h_{baro}
Air data system	$-$ V_a

Simulated angular accelerometer data were obtained by differentiating the rate gyro data. Simulated magnetometer data were obtained using the equations

$$\begin{bmatrix} B_x \\ B_y \\ B_z \end{bmatrix} = \begin{bmatrix} c\theta c\psi & c\theta s\psi & -s\theta \\ s\varphi s\theta c\psi - c\varphi s\psi & s\varphi s\theta s\psi + c\varphi c\psi & s\varphi c\theta \\ c\varphi s\theta c\psi + s\varphi s\psi & c\varphi s\theta s\psi - s\varphi c\psi & c\varphi c\theta \end{bmatrix} \begin{bmatrix} B_{x_0} \\ 0 \\ B_{z_0} \end{bmatrix}. \quad (42)$$

Here, the values of B_{x_0} and B_{z_0} were taken to be those typical of the San Francisco Bay area (dip angle of 62°). The angles (φ, θ, ψ) were taken from the INS and directional gyro measurements.

The recorded data at each sample point (approximately 1.018 sec apart) consisted of an average of the 20 previous samples taken approximately every 0.05 sec. Thus, the data had some built-in smoothing and some inherent lag. No attempt was made to smooth the data further. Misalignments between the instrument axes, acceleration measurement effects due to displacement from the aircraft c.g., and other instrument errors were unknown. It was found that to obtain acceptable results, the bias and scale factor corrections which appear in Table 1 had to be made to the linear accelerometer measurements.

TABLE 1.- CORRECTIONS TO CV-990 LINEAR ACCELEROMETER
MEASUREMENTS

ACCELEROMETER	BIAS - FT/SEC^2	SCALE FACTOR ERROR
f_x	2.39	-0.4098
f_y	0.21	--
f_z	-3.65	--

The three CV-990 flight sequences used to test the esti-
mators were·

(1) 400 sec of level flight, simulated approach (down to
90 ft altitude), and climbout, primarily longitudinal
motion.

(2) 150 sec of level coordinated turn of 180°; primarily
lateral motion.

(3) 250 sec of level flight, turn of 30°, simulated
approach, and climbout, combined longitudinal and
lateral motion.

Methods 1 and 2 were first tested using the above data
sequences. The performance was assessed, as mentioned before,
by examining the statistical differences between the estimated
attitude angles and those directly measured. There are obvious
discrepancies in these data besides the normal electronic noise.
There would exist some misalignment between the measured atti-
tude axes (X and Y of the LTN 51), the directional gyro
(Z axis), the rate gyro axes, and the linear accelerometer
axes. The accelerometer would sense all rate terms by not
being located on the aircraft center-of-gravity. The gyros
would have acceleration dependent terms and as mentioned above,
the accelerometers had large bias and scale factor errors.

To make the comparisons, Methods 1 and 2 were run using
the first two data sequences. For gain selection, it was
assumed that the input measurement noise had the following
standard deviations·

Angular accelerometers - $\sigma_{\dot{p}}$, $\sigma_{\dot{q}}$, $\sigma_{\dot{r}}$ - 0.002 rad/sec^2

Independent angle computations - σ_{φ_m}, σ_{θ_m}, σ_{ψ_m} - 0.02 rad.

Linear accelerometers - σ_{f_x}, σ_{f_y}, σ_{f_z} - 0.03 ft/sec^2

Altimeter - σ_h - 10 ft.

With these values, the gains were computed using Eqs. (41). They appear in Table 2. In addition, for Method 2, the following constants were used in the process of computing the angle-of-attack α_m [5] (see Eq. (3)):

m = 5652.2 slugs

C_{Z_α} = 5.15662 -

S = 2250 ft^2

$k_{\alpha 1}$ = 0.09 rad

$k_{\alpha 2}$ = -0.13674 -

TABLE 2. FILTER GAINS FOR INITIAL TESTS OF METHODS 1 AND 2

	BIAS GAIN k_B	RATE GAIN k_1	POSITION GAIN k_2
Altitude filter ($\dot{\hat{h}}$, $\hat{h}$)	0.03	0.2330	0.7493
Attitude filters ($\hat{p}, \hat{\varphi}, \hat{q}, \hat{\theta}, \hat{r}, \hat{\psi}$)	0.03162	0.2414	0.7634

For each run, the mean and standard deviation between the estimated attitude angles and those measured by the INS and directional gyro were computed. A comparison of these statistical quantities appears in Table 3.

For Sequence No. 1, the performance of both methods is acceptable, although the standard deviations in (φ, θ, ψ) are 30%-60% better with Method 2. The performances of both methods could be improved with gain adjustment.

For Sequence No. 2, Method No. 2 is substantially better than Method 1. The estimation algorithm in Method 1 is set so that whenever the angular rate magnitude becomes greater than

TABLE 3.- COMPARISON OF METHODS 1 AND 2 FOR THE FIRST TWO
CV-990 DATA SEQUENCES

SEQUENCE	ANGLE, DEG	METHOD 1		METHOD 2	
		m	σ	m	σ
1	φ	-0.52	1.38	-0.21	0.54
	θ	-0.86	1.66	0.42	0.98
	ψ	-1.13	2.75	0.82	2.03
2	φ	0.63	4.15	0.24	2.14
	θ	4.22	2.20	-0.93	0.54
	ψ	-7.24	3.72	0.56	3.98

a fixed limit, the pitch and roll angles are updated open-loop
by use of simulated (integrated) angular accelerometer infor-
mation. For the gyro data which was used to generate this
information, the noise and drift rates were probably too great
(i.e., the measured angular rates didn't match the measured
changes in INS angles) to allow good angular tracking, even
for only a two-minute span. Thus, Method 1, in its present
form, was judged not adequate for lateral transient tracking
with the given quality of rate information available on the
CV-990 flight.

There are probably modifications to Method 1 which would
improve performance. For example, the acceleration vector
used to track gravity could be modified to account for expected
reorientation caused by a turn. The estimator performance
could be improved with a better knowledge of the instrumenta-
tion errors. It also would be desirable to obtain more data
sequences and work with the raw data at each sample point
rather than data averaged over 20 samples.

At this point in the study, Methods 3 and 4 (discussed in
Chapter II) were introduced. Again, the motivation for Method
3 was to remove the ambiguity of the equations for determining
roll angle which exists in Method 2. The motivation for
Method 4 was to test the overall estimation concept using a
simpler set of instruments.

The two new estimator concepts were tested with the same
data sequences described previously. Comparisons of the
resulting means and standard deviations of the difference
between the measured and estimated roll, pitch, and heading
angles for Methods 2, 3, and 4 are presented in Table 4.

30

TABLE 4.- MEANS (m) AND STANDARD DEVIATIONS (σ) OF ESTIMATOR STATE ERRORS FOR THREE MECHANIZATIONS DURING THREE FLIGHT SEQUENCES

SEQUENCE	ANGLE, DEG	METHOD					
		2		3		4	
		m	σ	m	σ	m	σ
1	φ	-0.21	0.54	-0.40	1.31	-0.51	1.23
	θ	0.42	0.98	0.42	0.95	0.40	0.98
	ψ	0.82	2.03	0.94	1.48	0.97	1.51
2	φ	0.24	2.14	0.70	2.09	0.45	1.87
	θ	-0.93	0.54	-0.91	0.74	-0.91	0.32
	ψ	0.56	3.98	-0.07	2.29	0.57	1.98
3	φ	0.19	0.96	0.31	5.14	0.18	2.16
	θ	-0.84	2.24	-0.82	2.21	-0.88	2.05
	ψ	-1.48	4.94	-1.19	3.82	-1.49	3.37

The values shown in Table 4 only relate relative performance for the given set of filter gains and instrument calibration factors chosen for the particular runs. General improvements can be made by parameter adjustment as is discussed next. The Table 4 data show that not relying on the (simulated) magnetic field for computing the angle φ (Methods 3 and 4) resulted in an improvement in the standard deviation of the heading angle difference $\tilde{\psi}$. The pitch angle was generally unaffected by the estimator method used except during Sequence 2. Here, removing the simulated pitch angular accelerometer data (in Method 4) lowered the standard deviation of the pitch angle difference $\tilde{\theta}$. The mean and standard deviations of the roll angle difference $\tilde{\varphi}$ generally increased due to the assumptions of Methods 3 and 4, as would be expected.

A limited study was made to determine what improvements could be made to the performance by changing the model parameters used to compute α_0 as a function of flap angle and the complementary filter gains. Recall that Methods 2-4 use the computed angle-of-attack of Eq. (3). In this expression, f_{z_m} is the adjusted aircraft-fixed, downward component of measured acceleration equal to

$$f_{z_m} = (1 + \varepsilon_{a_{zc}})f_{z_m} + b_{a_{zc}} \qquad . \tag{43}$$

31

Here, ε_{azc} and b_{azc} are the scale factor and bias calibration terms. Thus, Eq. (3) has the parameters $k_{\alpha 1}$, $k_{\alpha 2}$, ε_{azc}, b_{azc} and $(m/C_{Z_\alpha}S)$ which can all be adjusted to affect the computed α_c and θ_c. For the data listed previously, the values of $k_{\alpha 1}$ and $k_{\alpha 2}$ were 0.09 and -0113674, respectively. A test was made using data input Sequence 1 with Method 2 and the values ($k_{\alpha 1}$ = -0.9; $k_{\alpha 2}$ = -0.095). This produced the results:

ANGLE, DEG	m	σ
φ	0.11	0.64
θ	-0.22	0.60
ψ	-0.39	1.28

By comparing these data with the results in Table 4, it can be seen that the mean errors were cut in half, and general improvement was realized in the standard deviations of θ and ψ. This indicates the importance of having a good knowledge of the aircraft model for α_o in Eq. (3). It is expected that additional improvement could be made by adjustment of the other instrument calibration quantities.

The previous data were produced based on the assumptions that the angular accelerometer measurements had noise with standard deviations of 0.002 rad/sec^2. It was also assumed that the angles measured from the magnetometers and by use of Eq. (3) had noise with standard deviations of 0.02 rad. The resulting Kalman gains produced filters with natural frequency of 0.3162 rad/sec. Another test was made in which this frequency was changed to 0.2 rad/sec by gain adjustment. The results were (again with Method 2 and Sequence 1)·

ANGLE, DEG	m	σ
φ	0.10	0.44
θ	-0.22	0.57
ψ	-0.39	1.09

Here, it is seen that each standard deviation is decreased somewhat compared to the previous data. Again, further improvement can be made by further gain adjustment.

For further comparison, the changes in $k_{\alpha 1}$, $k_{\alpha 2}$, and the filter gains were used also to regenerate results for Sequence 1 using Methods 3 and 4. The results are compared in Table 5 with those of Table 4. As can be seen in Table 5, these changes almost uniformly lowered all the mean differences and the associated standard deviations.

TABLE 5.- COMPARISON OF MEANS (m) AND STANDARD DEVIATIONS (σ) OF ESTIMATOR STATE ERRORS FOR SEQUENCE 1 WITH ORIGINAL AND MODIFIED FILTER PARAMETERS AND CONSTANTS $k_{\alpha 1}$ AND $k_{\alpha 2}$ (FLAP ANGLE EFFECT)

PARAMETERS	ANGLE, DEG	METHOD					
		2		3		4	
		m	σ	m	σ	m	σ
Original	φ	-0.21	0.54	-0.40	1.31	-0.51	1.23
	θ	0.42	0.98	0.42	0.95	0.40	0.98
	ψ	0.82	2.03	0.94	1.48	0.97	1.51
Modified	φ	0.10	0.44	-0.36	2.06	-0.55	1.06
	θ	-0.22	0.57	-0.21	0.57	-0.23	0.66
	ψ	-0.39	1.09	0	1.07	-0.03	0.93

From Tables 4 and 5, the following conclusions can also be made:

(1) The pitch angle accuracy is essentially independent of the estimator method used. Thus, for this data, no value is gained from use of the pitch angular accelerometer, as in Methods 2 and 3

(2) The roll angle estimates $\hat{\varphi}$ are generally more accurate in Method 2 in which the magnetic field is used to smooth both $\hat{\varphi}$ and $\hat{\psi}$. This is expected because the aircraft does not always obey the coordinated turn assumption which is inherent in Methods 3 and 4.

(3) The heading angle estimates $\hat{\psi}$ are closer to the directional gyro measured values when the roll angle estimate $\hat{\varphi}$ is assumed to be a function of $\dot{\hat{\psi}}$

33

(Methods 3 and 4). This is presumed to be due to an inherent disagreement between the INS and the directional gyro measurements.

(4) Method 4 produces essentially equivalent accuracy to Method 3. Thus, Method 4 is preferred to Method 3 for this data because one additional rate sensor (the roll angular accelerometer) can be omitted.

Plots comparing the estimated and measured roll, pitch, and heading angles using Method 2 on data Sequence No. 1 are shown in Fig 7. The agreement is good despite the relatively "noisy" aircraft trajectory. It can be concluded that the nonlinear estimators work well using actual flight data. Based on the limited data trials, it appears that they provide angle estimates that are adequate for flight control.
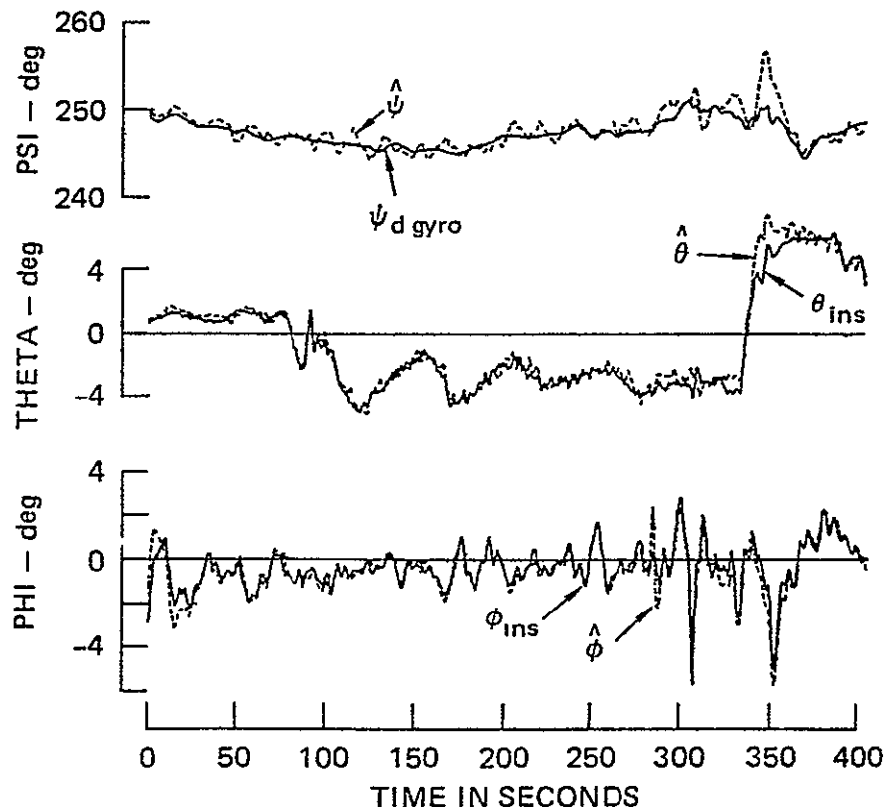
FIGURE 7.- METHOD 2 ESTIMATED ORIENTATION ANGLES FOR
DATA SEQUENCE NO 1

34

Cessna 402B Performance Results

Towards the end of this study, a small amount of data (80 sec period) became available which had been collected on the Ames Cessna 402B aircraft. These data were collected during the final approach and landing portion of a May 1977 flight at Crows Landing, California. This portion of the flight was reported to be subject to high lateral winds such that noticeable sideslip conditions prevailed. However, the INS measurements of wind magnitude and direction were not functional for this flight. Furthermore, the collected data had a high content of spikes and data dropouts. These anomalies were removed by interpolation and other manual techniques to make the data usable.

It was highly desirable to use these data for further estimator investigation because actual magnetometer data were recorded. Furthermore, all three attitude angles were measured and available from the INS system. (Recall that for the CV-990 data, heading angle was taken from a directional gyro, and magnetometer measurements were artificially generated.) Thus, these new data could produce new insights.

A serious problem with the 402 data was the high error content of the baro-altimeter recording. The baro-altimeter is a key instrument for computing pitch angle in Methods 2-4. Thus, it was decided to modify the program so that pitch angle wasn't estimated, but instead it was read directly from the INS. Thus, in the subsequent tests, only the roll and heading angles were estimated. However, this was still significant because it represented using actual magnetometer data to determine both roll and heading angles.

The instrumentation that is available on the Ames 402B is listed in Table 6. Also listed is the output range of the instruments, the number of digits recorded, and the equivalent accuracy. Details of this flight data system and its calibration can be found in Ref. 13. Again, as with the CV-990 system, the relative alignments of the three-axis instrument packages were unknown. Also, the locations of the linear accelerometers with respect to the aircraft center of gravity were unknown.

For the 402B flight, the sample period was 0.0702249 sec which represented a rate of about 14 samples per second. Initially, no instrument correction terms were included in the data processing. Gains were held the same as those used for generating Table 5.

TABLE 6.- INSTRUMENTATION CHARACTERISTICS OF AMES
CESSNA 402B [13]

INSTRUMENT	UNITS	FULL SCALE READING	BITS	EQUIVALENT GRANULARITY
Rate gyros (p,q,r)	deg/sec	± 15	10	0.029°/sec
INS angles (φ,θ,ψ)	deg	± 180	14	0.022°
Linear Accelerometers (f_x, f_y, f_z)	g	± 0.5 (f_x, f_y) ± 3.0 (f_z)	10	0.0040g = 0.03 ft/sec 0.0059g = 0.19 ft/sec
Magnetometers (B_x, B_y, B_z)	Gauss	± 600	10	1.17 Gauss
Altimeter (h_{baro})	ft	-1000 +9000	10	9.78 ft
Airspeed (V_a)	kts	250	10	0.244 kt = 0.41 ft/sec
Control Surfaces (δF, etc.)	deg	Full surface deflection (0°-45°)	10	0.044°

Figure 8 shows the initially estimated and INS measured
roll and yaw angles for the 80 sec segment of the 402B flight
using Method 2. As can be seen for this run, the estimated
angles follow the same trends as the INS measured angles. How-
ever, there is a large bias in the estimated roll angle. Also,
the estimated heading angle increasingly deviates from the
measured value as the angle becomes closer to 0°. For this ini-
tial test, the mean differences and associated standard devia-
tions between estimated and measured roll and heading angles were·

ANGLE, DEG	m	σ
φ	6.39	1.82
ψ	3.54	8.43

36
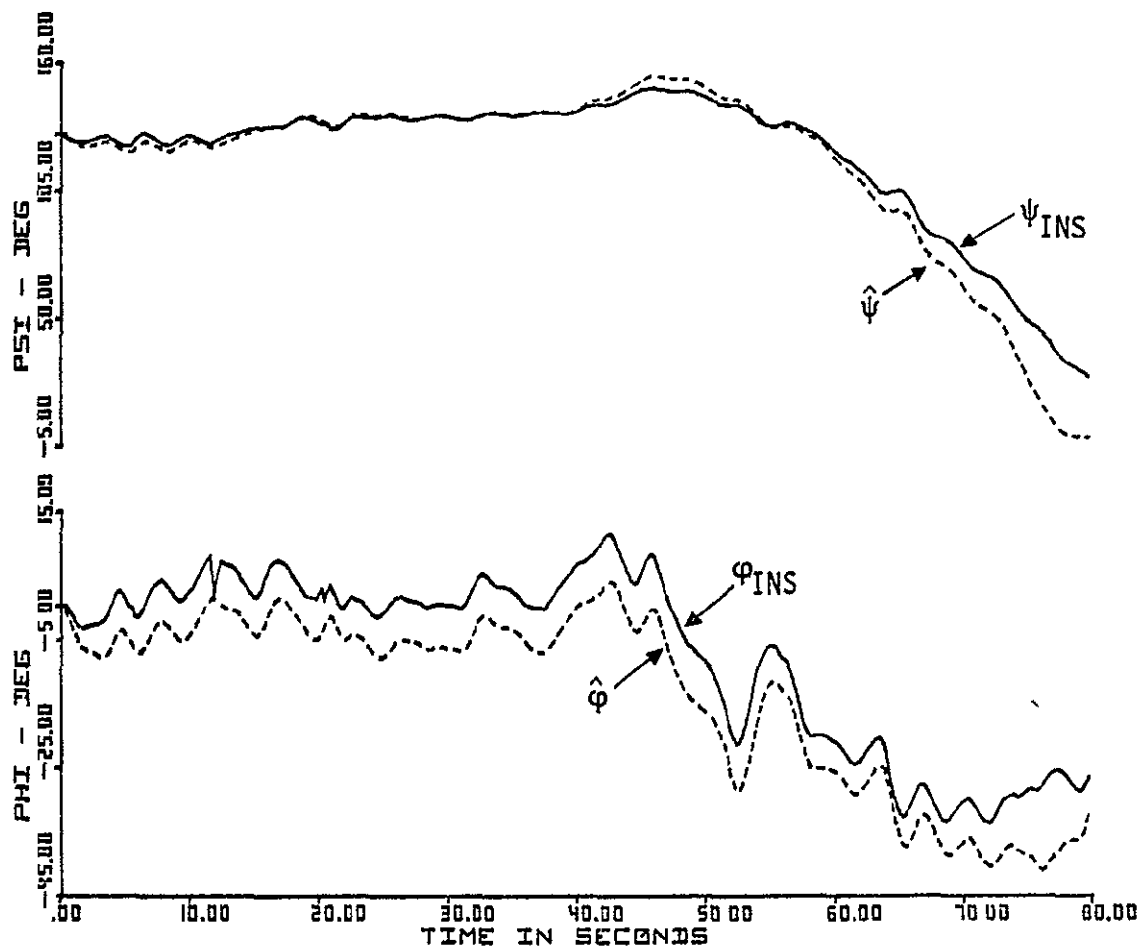
FIGURE 8.— INITIAL ESTIMATED AND MEASURED ROLL AND HEADING
ANGLES FROM CESSNA 402B DATA

It was concluded that signals of the three-axis magnetometer
(which is mounted in the vertical stabilizer of the 402B) were
being distorted by the aircraft structure, and that corrections
should be made.

The magnetometer data were examined at discrete points
along the trajectory and compared to the corresponding INS
measurements. It was determined that the characteristics of
the distortions were such that the signals were subject to both
misalignment and scale factor errors. Some calibration calcu-
lations were made using discrete points of the data, and the
resulting preliminary error magnitudes were determined to be:

Misalignment $(\psi_B, \theta_B, \varphi_B) = 1.9°, 1.2°, 6.6°$,

Scale factor error $(\varepsilon_{cbx}, \varepsilon_{cby}, \varepsilon_{cbz}) = -0.15, 0, -0.05$.

37

Corresponding correction terms were placed in the esti-
mator software to remove these errors. The data were repro-
cessed (again using Method 2) and the results are shown in
Fig. 9. The resulting means and standard deviations were

ANGLE, DEG	m	σ
φ	0.005	1.58
ψ	-0.336	1.38

As can be seen, this is a substantial improvement. A closer
match could be made between the estimated and INS measured
angles by further adjustment of gains and error correction
terms. It again can be concluded that this method of estimat-
ing attitude angles potentially works extremely well. The
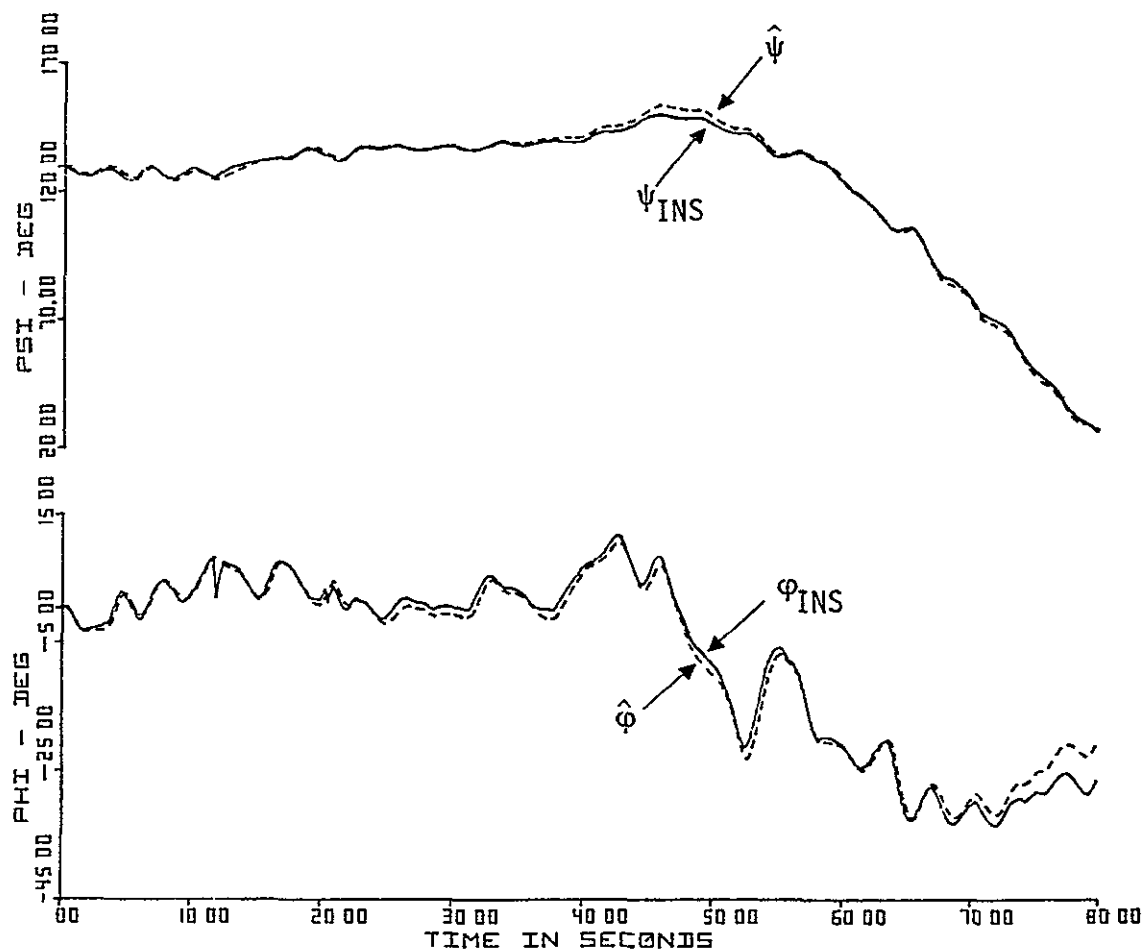
FIGURE 9.- ESTIMATED AND MEASURED ROLL AND HEADING ANGLES
WITH MAGNETOMETER DATA CORRECTIONS

38

method is tolerant to typical instrument misalignment errors. A reservation is that these results were obtained by assuming that pitch angle was known exactly.

The same data sequence was processed using estimator Methods 3 and 4. A comparison of the statistical results appears in Table 7. As can be seen from these results, Method 2 performs significantly better than Method 3. In turn, Method 3 performs significantly better than Method 4. The performance obtained from Method 4 is unacceptable. Thus, it is concluded that:

(1) In this flight sequence, where frequent attitude transients and sideslip conditions prevail, the coordinated turn assumption is continually violated. Thus, inherent errors are present in Methods 3 and 4. Significant information is obtained from the magnetometer data in Method 2 for directly computing the roll angle.

(2) In the presence of consistent attitude transients, the estimated roll rate ($\hat{p}$) information (Methods 2 and 3) becomes more important. The equations used to derive Method 4 include the assumption that p is negligible. (A possible fix would be to rotate the single rate gyro so that components of both roll rate and yaw rate are measured.)

It is certainly possible that the performance achieved from Methods 3 and 4 could be improved by gain changes and software modifications. However, such efforts should await more extensive flight data to work with.

TABLE 7.- COMPARISON OF ESTIMATOR METHODS USING THE
402B DATA

ANGLE, DEG	METHOD					
	2		3		4	
	m	σ	m	σ	m	σ
φ	0	1.58	-0.20	4.56	0.23	10.55
ψ	-0.034	1.38	0.12	4.30	-1.81	25.03

Conclusion

Based on the results of processing the CV-990 and Cessna 402B data, it is concluded that Method 2 is the preferred estimator structure. Modification can be made to this method so that the complementary filter software which determines pitch angle can be eliminated. That is, pitch angle can be computed directly by using Eqs. (3) and (10). This also eliminates need of the pitch accelerometer.

Also based on these results, it can be concluded that one can potentially estimate the three orientation angles of the aircraft to a high degree of accuracy. The estimated roll and heading angle trajectories obtained using the Cessna 402B data resembled very closely the angles directly measured using the INS. This is very encouraging. The possible problems which may arise due to the ambiguity in solution for roll angle in Method 2 will have to be discovered or dismissed by much more extensive flight testing.

IV

SOFTWARE MECHANIZATION REQUIREMENTS

An essential requirement for mechanizing the state esti-
mator concepts is that their software can be successfully
coded in a typical microcomputer with the associated con-
straints on memory, computation accuracy, and cycle time. To
make an assessment of to what degree this requirement can be
met, the following study was made using a DEC PDP 11/70 com-
puter.

First, the FORTRAN software required to mechanize the
Method No. 2 state estimator was extracted from the ESTEST
program described in Appendix A. (The ESTEST program was
developed to test all estimator configurations using flight
data.) The Method 2 estimator configuration is the longest
but most accurate of the configurations studied. The Method
2 FORTRAN code is presented and explained in Appendix B.

Next, the portion of the software which represents com-
putations made every cycle of the mechanized estimator were
recoded on the PDP 11/70. Phases of these computations
include:

(1) modification of sensor readings to remove known
errors;

(2) computation of independent measures of the attitude
angles (φ, θ, ψ) from magnetometer and other
readings; and

(3) primary state estimator (filter) computations.

Also, there would be a small amount of additional software
for input and output conversion. The program was coded using
the C language of the UNIX system (developed by D.M. Ritchie,
Bell Laboratories) which provides efficient, compact PDP 11
code. A listing of the C source deck is also presented in
Appendix B.

The C source deck was compiled and assembled into PDP 11
machine language using the floating point instruction set
The associated memory requirements for this program were 2024_{10}
sixteen bit words. This requirement could be reduced about 25%
using fixed point arithmetic. However, fixed point arithmetic
would require addition of some scaling operations.

Some additional software would be required to make the
initial computations at the beginning of use of the estimator.

These computations are presented in Appendix B. Also, executive logic would be required to sample and scale the A/D buffer inputs, to interface with pilot inputs, to prepare the estimate outputs for display or digital control, and to control program cycling. A conservative estimate is that this would add 50% to the memory requirements. Thus, it is seen that the read only memory (ROM) requirements for mechanization are much less than 4096 (4K) sixteen-bit words. With efficient coding, this could be reduced to 2K words.

The variable storage requirements (RAM) for mechanization is 132_{10} sixteen-bit words. Thus, a 256 x 16-bit RAM unit is adequate.

The tests made using the Cessna 402 discussed in the previous chapter used data with ten-bit accuracy. The estimate results were quite adequate in comparison to INS measurements. Thus, it can be concluded that a microcomputer with twelve or sixteen-bit words is adequate for mechanizing the state estimator. Further tests would be required to evaluate the adequacy of an eight-bit processor.

To obtain an estimate of computation time, a single pass through the PDP 11 computations was timed. The result was less than 16 7 msec. (The minimum measurable time increment is 1/60 sec.) Norden Corporation personnel estimated that the time increase would be a factor of five (to less than 83.5 msec) for running on the LSI11M microcomputer which uses the PDP 11 code. The LSI11M is a ruggedized microcomputer suitable for airborne application.

For processing the flight test data, sample rates of once per second (CV-990 data) and fourteen times per second (C-402 data) were used. The Method 2 estimator worked well in both cases. Thus, a sample rate of five times/sec appears to be adequate.

If the cycle time were set at 200 msec so that the sensors were sampled five times/sec, it is seen that the basic computations of the state estimator would require only 41% of real time for the LSI11M Again, to be conservative, this value could be increased 50% to account for additional executive computations. There appears to be plenty of margin for running time.

The above study is a first approximation to the microcomputer mechanization requirements. From these, it can be concluded that the state estimator concept can easily be mechanized in existing microcomputers. To obtain more precise timing and memory requirements requires actual mechanization on a microcomputer with additional software added for driving A/D converters, displays, and the program control logic.

V

SUMMARY, CONCLUSIONS, AND RECOMMENDATIONS

Summary

This study has accomplished the following:

(1) Four nonlinear state estimators (Methods 1, 2, 3, and 4) were devised which provide techniques for obtaining the angular orientation of the aircraft. These techniques are alternatives to direct measurement by use of vertical and directional gyros. These estimators have the potential of being of low cost and of high reliability by implementation using solid state instruments (pressure sensors, accelerometers, magnetometers) and the microcomputer.

(2) An extensive FORTRAN computer program was developed to demonstrate and evaluate the estimators by processing recorded flight test data. This program simulates the estimator operation and it compares the state estimates with actual state measurements. Full details and capabilities of this program are presented in Appendix A.

(3) The above program was used to evaluate the four state estimator configurations with limited data recorded on the NASA Ames CV-990 and Cessna 402B aircraft. Three of the configurations worked reasonably well with the CV-990 data and Method 2 worked well with the 402B data. From these evaluations, the preferred state estimator configuration was chosen.

(4) A preliminary assessment was made of the requirements for implementing the selected state estimator on a typical microcomputer.

Conclusions

Based on limited flight data analysis, it is concluded that the estimator concept of determining attitude angles without direct measurement has definite potential to provide low-cost flight control The measurements required to estimate roll, pitch, and yaw angles include the three components of magnetic field (B_x, B_y, B_z), three components of linear acceleration (f_x, f_y, f_z), two components of angular acceleration ($\dot{p}$, $\dot{r}$), true airspeed (V_a), baro-altitude (h), and

possibly flap angle (δF). Angular acceleration could be re-
placed by angular rate (p, r) measurements. Altitude and true
airspeed measurements can be obtained by processing static
and dynamic pressure data.

It is furthermore concluded that the above set of measure-
ments, which are smoothed by nonlinear filtering in the esti-
mator, can provide attitude angle estimates to a high degree
of accuracy. For example, during an 80 sec run using Cessna
402B data, the roll angle excursions of the aircraft exceeded
45° and the yaw angle excursions exceeded 120°. During this
time, the estimated roll angle matched the INS measured roll
angle to a mean of 0° and a standard deviation of 1.6°. The
estimated yaw angle matched the INS measured yaw angle to a
mean of -0.3° and a standard deviation of 1.4°. This accuracy
is more than adequate for flight control purposes.

The selected state estimator configuration (Method 2) has
a potential ambiguity problem in determining roll angle when
the aircraft is flying at a magnetic heading of nearly North
or South. This problem was not encountered with the limited
data processed in this study. The solutions to this problem
(encompassed in Methods 3 and 4) degrade the estimator perfor-
mance in the presence of aircraft transient attitude motion.
The degree of degradation is dependent upon the instrumentation
errors and the amount of disturbances causing transient motion
of the aircraft.

The computation mechanization requirements for implement-
ing the Method 2 state estimator are easily met with today's
microcomputers. Preliminary conservative estimates are that
to code this estimator on a ruggedized microcomputer requires
less than 4K x 16-bit ROM memory and less than 256 x 16-bit RAM
memory. Twelve-bit memory is also sufficient. A preliminary
timing assessment indicated that less than 0.1 sec is required
to cycle the estimator equations on the ruggedized microcomputer.
This allows a sample rate of five/sec with plenty of time to
spare for either driving displays or automatic control actua-
tion.

Recommendations

The results of this study were based on limited flight
data. The data collected did not represent all the flight
regimes in which the estimators would potentially have to
operate. In particular, flight data in which several turns,
intentional lateral and longitudinal perturbations, known wind
shears, stalls, and engine-out conditions were not tested. It

44

is recommended that such data be collected on the Cessna 402B aircraft and that a more thorough investigation be made.

It is also recommended that the following steps be taken

(1) Estimator Methods 2, 3, and 4 are based on computing pitch angle from measurements of vertical accelera- tion, dynamic pressure, and flap angle and estimates of aircraft mass and lift coefficient. Study should be directed to find a more direct procedure to compute pitch so that at least flap angle measure- ments could be eliminated.

(2) Estimator Method 2 gave the best results in the studies made. However, it has a potential ambiguity problem in computing roll angle when the aircraft is flying with a magnetic heading of near 0° or 180°. This potential problem must be thoroughly investigated with flight test data, and further corrective logic may be required.

(3) Intentional instrumentation errors should be artifi- cially introduced into the program used to process the flight data and to evaluate the estimators. The sensitivity of the state estimator outputs to instru- ment error magnitude can then be determined. This procedure is suitable for specifying required instru- ment accuracy. These results would complement laboratory studies of existing low-cost solid state sensors.

(4) A typical microcomputer should be selected along with appropriate sensor interface equipment, recording equipment, and operating peripherals. Additional software should then be developed to sample the sensor input, provide program control, and drive outputs for data recording (or display). The entire software code of the selected estimator configuration should then be loaded into the microcomputer, and subsequent tests should be made to obtain more definitive require- ments for computer mechanization.

Further concept study of low-cost state estimation for flight control should produce

(1) A precise definition of the desired state estimator configuration and any limitations it has.

(2) The computer, sensor, and display mechanization requirements to realize this concept. These include accuracy requirements of both the computer and sensors

45

APPENDIX A

PROGRAM USER'S GUIDE

As part of this study effort, a FORTRAN digital computer program (ESTEST) was developed for the Ames IBM 360 to process the flight data. The purpose of this program is to simulate operation of the state estimators used for flight control purposes. The flight data serves as input to drive this simulation. The state estimates are compared to actual state variables obtained by direct measurement to assess the estimator performance.

The ESTEST program allows the user to make the following studies:

(1) Digital implementation of the state estimator can be checked.

(2) Different estimator formulations can be tested and compared.

(3) Performance of the estimator can be measured for different flight conditions and sensor accuracies.

(4) Gains and other program variables can be adjusted.

(5) Airborne computer requirements for mechanization can be partially assessed.

This appendix serves as a user's guide for ESTEST. It is organized as follows.

(1) The input variables are defined, and a sample input deck is listed.

(2) The program output is explained, and sample outputs are presented.

(3) The general capabilities and organization of the program are explained.

Input Variables

Five input formats are used to read in the initial data and program control variables. These formats are.

47

(1)   FØRMAT(2X,5I3),
(2)   FØRMAT(20A4),
(3)   FØRMAT(2X,6I3),
(4)   FØRMAT(6I6), and
(5)   FØRMAT(2X,6E12.5).

Twenty-eight input data cards are read using these formats to initialize operation of the program. They are presented in Table A.1 as they are arranged in the data card set; the above formats are referenced. The definitions of these variables are presented in Table A.2. Figure A.1 shows a listing of a typical input deck, with the appropriate Ames IBM 360 control cards.

After the initialization data and control variables have been read in, ESTEST immediately prints this data. This is discussed in the next section. Then, certain initialization computations are made such as conversion from degrees to radians. Then, the time data set is read sequentially using the following FORTRAN statements·

```
      READ(8) NTIME
   50 CONTINUE
      READ(8) K,(CVDAT(J),J=1,17)
      IF (K.LT.NST) GØ TØ 50.
```

This is explained as follows:

(1)   The number of time points of data in the data set (NTIME) is first read.

(2)   Each sequential data time point record is then read until the index K is equal to the input quantity NST which is the start point desired.

The quantities in each data time record represented by the array CVDAT are defined in Table A.3. The program is set by the logic variable NF1 so that either data collected on the CV-990 aircraft or the Cessna 402B aircraft can be used. The differences beween the CV-990 and C-402 data arrays are indicated in Table A.3.

Program Output

The first thing the program does after reading in the run initialization data is to print it. A sample of this printout is shown in Fig. A.2. Each of the variables is defined by the preceding acronym which is defined in Table A.2.

48

TABLE A.1 – SEQUENCE OF INITIAL DATA AND PROGRAM CONTROL VARIABLES READ TO INITIALIZE ESTEST OPERATION

CARD	FORMAT	FORTRAN ACRONYMS
1	1	(IDATE(I),I=1,3), NR, NAC
2	2	(ALPHA(I),I=1,20)
3	3	NF1, NF2, NF3, NF4, NF5, NF6
4	3	NF7, NF8, NF9, NF10, NF11
5	4	NS, NST, NRU, IX
6	5	BMAG, DL1, DL2
7	5	FIB, THB, SIB, SIBY, THBZ, FIBZ
8	5	BBX, BBY, BBZ, EPBX, EPBY, EPBZ
9	5	SGBX, SGBY, SGBZ
10	5	DT, TSTØP, TI, DTP, DTPL, DTST
11	5	FIPD, THPD, SIPD, EPPD, EPQD, EPRD
12	5	BPD, BQD, BRD, SGPD, SGQD, SGRD
13	5	BV, EPV, SGV
14	5	FIA, THA, SIA, XA, YA, ZA
15	5	BAX, BAY, BAZ, EPAX, EPAY, EPAZ
16	5	SGAX, SGAY, SGAZ
17	5	BH, EPH, SGH
18	5	FIAM, THAM, SIAM, XAM, YAM, ZAM
19	5	THV, RKU, RKSB, RKB, DFBI, DFSF
20	5	FIAL, THAL, SIAL, RKA1, RKA2
21	5	RL, RKGX, RKGY, RKGZ, RKB1
22	5	FGL, G
23	5	SICBX, THCBX, SICBY, FICBY, THCBZ, FICBZ
24	5	RM, CZAL, SW, ALZRØ, ALZR1, HØ
25	5	RK1, RK2, RK3, RK4, RK5, RK6
26	5	RK7, RK8, RKBH, RKBP, RKBQ, RKBR
27	5	BAXC, BAYC, BAZC, EAXC, EAYC, EAZC
28	5	BCBX, BCBY, BCBZ, ECBX, ECBY, ECBZ

TABLE A.2.- DEFINITION INPUT DATA CARD VARIABLES LISTED
IN TABLE A.1

CARD	ACRONYM	SYMBOL	DEFINITION
1	IDATE(I)	~	Date in month/day/year that data were taken
	NR		Estimator (or run) trial number
	NAC		Type of aircraft (i.e., 990, 402).
2	ALPHA(I)		120 characters used to identify a particular run
3	NF1		Data source: 1 - CV-990 2 - C-402B
	NF2		Magnetic data used: 1 - Computed from INS angles 2 - Actual magnetometer
	NF3		Simulated sensor errors introduced: 0 - None 1 - Deterministic 2 - Deterministic + random
	NF4 ι		Sensor corrections used: 0 - None 1 - Corrections
	NF5		Airspeed measurement source: 1 - Pitot tube 2 - J-Tek sensor
	NF6		Method of computing φ, θ, and ψ: 1 - Method 1 2 - Method 2 3 - Method 3 4 - Method 4
4	NF7		Computer printout: 0 - None 1 - Major 2 - Major + secondary
	NF8		Computer plot: 0 - No plot 1 - Plot

CARD	ACRONYM	SYMBOL	DEFINITION
4	NF9		Ames Zeta plot: 0 - No plot data 1 - Plot data saved
	NF10		Statistical measures: 0 - Not computed 1 - Computed
	NF11		φ, ψ computations only: 0 - Option off 1 - Option on
5	NS		Number of samples to skip between use
	NST		Data set index number used to indicate start of data of interest
	NRU		Number of cases to be run from data set.
	IX		Initial add number for random number generator.
6	BMAG	B_{mag}	Assumed or actual magnitude of the local magnetic field (milligauss)
	DL1	δ_{L1}	Deviation of magnetic north from true north (deg)
	DL2	δ_{L2}	Magnetic field dip angle (deg)
7	FIB THB SIB	φ_B, θ_B ψ_B	Simulated magnetometer misalignment angles (deg)
	SIBY THBZ FIBZ	ψ_{By}, θ_{Bz}, φ_{Bz}	Simulated magnetometer skew angles; B_y with respect to B_x and B_z with respect to B_x-B_y plane (deg)
8	BBX BBY BBZ	b_{Bx}, b_{By}, b_{Bz}	Simulated biases of magnetometer readings (milligauss)
	EPBX EPBY EPBZ	ε_{Bx}, ε_{By}, ε_{Bz}	Simulated magnetometer scale factor errors; $(1+\varepsilon)$ multiplies the simulated signal

CARD	ACRONYM	SYMBOL	DEFINITION
9	SGBX SGBY SGBZ	σ_{Bx}, σ_{By}, σ_{Bz}	Standard deviations used by random number subroutine for simulated magnetometer noise (milligauss)
10	DT	Δt	time between samples (sec)
	TSTOP	t_{stop}	Length of time duration of data sequence used in the run (sec)
	TI	t_I	Time from beginning of data record to point where run begins; corresponds to NST (sec)
	DTP	Δt_p	Print interval (sec)
	DTPL	$\Delta t_{p\ell}$	Plot interval (sec)
	DTST	Δt_{st}	Interval for computing estimate deviation means and variances (sec)
11	FIPD THPD SIPD	φ_p^*, θ_p^*, ψ_p^*	Simulated angular accelerometer misalignment angles (deg)
	EPPD EPQD EPRD	ε_p^*, ε_q^*, ε_r^*	Simulated angular accelerometer scale factor errors
12	BPD BQD BRD	b_p^*, b_q^*, b_r^*	Simulated angular accelerometer biases (rad/sec^2)
	SGPD SGQD SGRD	σ_p^*, σ_q^*, σ_r^*	Standard deviations used by random number subroutine for simulated angular accelerometer noise (rad/sec^2)
13	BV	b_v	Simulated airspeed measurement bias (ft/sec)
	EPV	ε_v	Simulated airspeed measurement scale factor error
	SGV	σ_v	Standard deviation used by random number subroutine for simulated airspeed measurement noise (ft/sec)

CARD	ACRONYM	SYMBOL	DEFINITION
14	FIA THA SIA	φ_a, θ_a, ψ_a	Simulated linear accelerometer mis-alignment angles (deg)
	XA YA ZA	x_z, y_a, z_a	Simulated position of linear acceler-ometers with respect to the aircraft c.g.
15	BAX BAY BAZ	b_{ax}, b_{ay}, b_{az}	Simulated linear accelerometer biases (ft/sec^2)
	EPAX EPAY EPAZ	ε_{ax}, ε_{ay}, ε_{az}	Simulated linear accelerometer scale factor errors
16	SGAX SGAY SGAZ	σ_{ax}, σ_{ay}, σ_{az}	Standard deviations used by random num-ber subroutine for simulated linear accelerometer measurement noise (ft/sec^2)
17	BH	b_h	Simulated altimeter bias (ft)
	EPH	ε_h	Simulated altimeter scale factor error
	SGH	σ_h	Standard deviation used by random num-ber subroutine for simulated altimeter measurement noise (ft)
18	FIAM THAM SIAM	φ_{am}, θ_{am}, ψ_{am}	Linear accelerometer misalignment cor-rection angles (deg)
	XAM YAM ZAM	x_{am}, y_{am}, z_{am}	Linear accelerometer position correc-tion terms with respect to the c.g. (ft)
19	THV	θ_v	Pitot tube misalignment correction angle (deg)
	RKU	K_u	Gain for airspeed filtering
	RKSB	K_{SB}	Gain for filtering $\hat{g} \times \hat{B}$ terms in Method 1

CARD	ACRONYM	SYMBOL	DEFINITION
19	TKB	K_B	Gain for filtering $\hat{B}$ in Method 2
	DFBI	$b_{\delta F}$	Flap angle bias (deg)
	DFSF	$\varepsilon_{\delta F}$	Flap angle scale factor error.
20	FIAL THAL SIAL	φ_α, θ_α, ψ_α	Angular accelerometer misalignment correction angles (deg)
	RKA1 RKA2	K_{a1}, K_{a2}	Extra gains
21	RL	r_L	Turn rate limit for update of $\hat{g}$ in Method 1 (rad/sec)
	RKGX RKGY RKGZ	K_{gx}, K_{gy}, K_{gz}	Gains for updating $\hat{g}$ from linear accelerometer readings in Method 1
	RKB1	K_{b1}	Gain used by digital lag network to smooth rate gyro data
22	FGL	$f_{g\ell}$	Threshold limit on accelerometer readings used to compute g in Method 1 (ft/sec^2)
	G	g	Normal gravity value (ft/sec^2)
23	SICBX THCBX SICBY FICBY THCBZ FICBZ	ψ_{Bx}, θ_{Bx}, ψ_{By}, φ_{By}, θ_{Bz}, φ_{Bz}	Magnetometer axis misalignment correction angles (deg)
24	RM	m	Aircraft mass (slugs)
	CZAL	$C_{Z\alpha}$	Aircraft lift coefficient as a function of angle-of-attack
	SW	S	Aircraft wing reference area (ft^2)

CARD	ACRONYM	SYMBOL	DEFINITION
24	ALZRO ALZR1	α_0, α_1	Terms used to compute zero lift angle-of-attack as a function of flap angle (rad, rad/rad)
	HØ	h_0	Barometric altimeter correction (ft)
25	RK1-RK6	K_1-K_6	Primary filter gains for estimating altitude, roll, and pitch (or angle-of-attack)
26	RK7, RK8	K_7, K_8	Primary filter gains for estimating yaw
	RKBH RKBP RKBQ RKBR	K_{bh}, $K_{b\dot{p}}$, $K_{b\dot{q}}$, $K_{b\dot{r}}$	Primary filter gains for estimating biases in altitude, roll acceleration, pitch acceleration, and yaw acceleration
27	BAXC BAYC BAZC	b_{axc}, b_{ayc}, b_{azc}	Linear accelerometer bias correction terms (ft/sec^2)
	EAXC EAYC EAZC	ε_{axc}, ε_{ayc}, ε_{azc}	Linear accelerometer scale factor correction terms
28	BCBX BCBY BCBZ	b_{cbx}, b_{cby}, b_{cbz}	Bias corrections to magnetometer signals (milliguass)
	ECBX ECBY ECBZ	ε_{cbx}, ε_{cby}, ε_{cbz}	Magnetometer scale factor error corrections

```
    LOGON FS  25,  1       ,  , SORE S  M,  STOP  17
FE  E 45  ATE
ULFF FT   001,,DATA    102 MA2MD
AMES  SYSLIB
CALL ESTSTS
    5   5  /7  1402
    FIRST TEST OF 402 DATA - LANDING PHASE OF FLIGHT
    2   2   0   1   2   2
    2   1   0   1   1
              1     1    333
  1.              19.            65.
  0.
  0.
  0.
  0.70225E-01 3.51125      0.0         0.70225E-01 0.70225E-01 0.70225E-01
  0.
  0.
  0.
  0.
  0.
  0.
  0.
  0.
  0.            0.5         0.5         0.5        79.0        0.5
  0.
                                                   4.0
  0.            32.172
  0.
  192.714       1.          105.72
  0.235         0.7493      0.09657     0.48284     0.09657     0.48284
  0.09657       0.46284     0.03        0.008       0.008       0.008
  0.
  0.
%END
  LOGOFF
```

FIGURE A.1.- LISTING OF TYPICAL ESTEST INITIAL DATA INPUT DECK

56

TABLE A.3.- QUANTITIES IN THE DATA INPUT ARRAY CVDAT

NO.	SYMBOL	DEFINITION (CV-990)	ALTERNATE DEFINITION (C-402)
1	t	Time (sec)	
2	φ	INS roll angle (deg)	
3	θ	INS pitch angle (deg)	
4	ψ	Dir. gyro yaw angle (deg)	ψ - INS yaw angle (deg)
5	p	Roll rate (deg/sec)	
6	q	Pitch rate (deg/sec)	
7	r	Yaw rate (deg/sec)	
8	h	Altitude (ft)	
9	V_a	J-Tek true airspeed (kts)	
10	γ	Flight path angle (deg)	B_x - Longitudinal magneto-meter reading (milli-gauss)
11	f_x	Longitudinal acceleration (ft/sec^2)	
12	f_y	Side acceleration (ft/sec^2)	
13	f_z	Vertical acceleration (ft/sec^2)	
14	W_{ind}	Wind magnitude (kts)	B_y - Lateral magnetometer reading (milligauss)
15	α_w	Wind angle (deg)	B_z - Vertical magnetometer reading (milligauss)
16	δF	Flap angle (deg)	δF_L - Left flap angle (deg)
17	δT	Throttle setting (%)	δF_R - Right flap angle (deg)

```
SNJAB,RUN2,J0
TSS 9.0 PTF49A
 BSN=9154 LOGON AT 14:11 ON 07/01/77
SYSTEM SPLIT 1730 7/1, SHUTDOWN 2300, AVAILABLE 7/2 0800 TO 1800, DOWN SUN, HOLIDAY MON 7/4, AVAILABLE AFTER 2200.
ETNEWS *UPDATE
DEF FT08F001,,DATA,CF402,MA2MO
MES USYSLIB
ALL ESTSTS*
 SECOND TEST OF 402 DATA * LANDING PHASE OF FLIGHT


ESTIMATOR TRIAL NUMBER  1 BASED ON RECORDED DATA TAKEN ON  5/ 5/77FROM THE   402 AIRCRAFT,


   DATA INPUT


NF1:  2  NF2:  2  NF3:  0  NF4:  1  NF5:  2  NF6:  2
NF7:  0  NF8:  1  NF9:  0  NF10: 1  NF11: 1
NS:  0  NRU:  1  IX:  333  N8T:  675
```

```
BHAG: 1.00000E 00  DL1:=1.00000E 01  DL2: 6.50000E 01
F18:    0.00000  THR:    0.00000  S18:    0.00000  SBY:    0.00000  T8Z:    0.00000  F8Z:    0.00000
BRX:    0.00000  RRY:    0.00000  RBZ:    0.00000  EPBX:   0.00000  EPBY:   0.00000  EPBZ:   0.00000
SGBX:   0.00000  SGBY:   0.00000  SGBZ:   0.00000
DT: 7.02249E-02  TSTP: 4.50000E 01  TI: 4.73300E 01  DTP: 7.02249E-02  DTPL: 4.91570E 01  DTST: 7.02249E-02
FIPD:   0.00000  THPD:   0.00000  SIPD:   0.00000  EPPD:   0.00000  EPQD:   0.00000  EPRD:   0.00000
PPD:    0.00000  RQD:    0.00000  BRD:    0.00000  SGPD:   0.00000  SGQD:   0.00000  SGRD:   0.00000
RV:     0.00000  EPV:    0.00000  SGV:    0.00000
FIA:    0.00000  THA:    0.00000  SIA:    0.00000  XA:     0.00000  YA:     0.00000  ZA:     0.00000
BAX:    0.00000  RAY:    0.00000  PAZ:    0.00000  EPAX:   0.00000  EPAY:   0.00000  EPAZ:   0.00000
SGAX:   0.00000  SGAY:   0.00000  SGAZ:   0.00000
RH:     0.00000  EPH:    0.00000  SGH:    0.00000
FIAM:   0.00000  THAM:   0.00000  SIAM:   0.00000  XAM:    0.00000  YAM:    0.00000  ZAM:    0.00000
THV:    0.00000  RKU: 5.00000E-01  RK8B: 5.00000E-01  RKB: 5.00000E-01  DFB: 7.90000E 01  DFSF: 5.00000E-01
FIAL:   0.00000  THAL:   0.00000  SIAL:   0.00000  RKA1:   0.00000  RKA2:   0.00000
RL:     1.00000  RKGV:   0.00000  RKGY:   0.00000  RKGZ:   0.00000  RKA1: 4.00000E 00
FGL:    0.00000  G: 3.21720E 01
SCBX: 1.90000E 00  TCBY:=1.20000E 00  SCRY:=1.90000E 00  FCBY: 6.60000E 00  TCBZ: 1.20000E 00  FCBZ:=6.60000E 00
RM: 1.92714E 02  CZAL: 1.00000E 00  SW: 1.95720E 02  AZR0:   0.00000  AZR1:   0.00000  HO:     0.00000
RK1: 2.33000E-01  RK2: 7.49300E-01  RK3: 9.65700E-02  RK4: 4.82840E-01  RK5: 9.65700E-02  RK6: 4.82840E-01
RK7: 9.65700E-02  RKA: 4.82840E-01  RKBH: 3.00000E-02  RKBP: 8.00000E-03  RKBQ: 8.00000E-03  RKBR: 8.00000E-03
BAXC:   0.00000  RAYC:   0.00000  BAZC:   0.00000  EAXC:   0.00000  EAYC:   0.00000  EAZC:   0.00000

BCRX:   0.00000  BCBY:   0.00000  BCBZ:   0.00000  ECBX:=1.50000E-01  ECBY:   0.00000  ECBZ:=5.00000E-02
```

FIGURE A.2.- PROGRAM PRINTOUT OF INPUT DATA

The program has the option (using the NF7 flag) of printing out no data, major data, or major plus secondary data every DTP seconds. The data heading and a sample of the printout data are shown in Fig. A.3. The major data are the first two lines at each time point. The secondary data are the next three lines. The acronyms shown in the data header define what the quantities in each data set are. These header acronyms are defined in Table A.4. The estimated quantities ($\hat{\phi}$, $\hat{\theta}$, $\hat{\psi}$, $\hat{p}$, $\hat{q}$, $\hat{r}$) in the second line of the printout appear directly below the measured quantities of the first line.

Another option which the program has (using the NF10 flag) is computation of statistical characteristics of the estimated variables ($\hat{\phi}$, $\hat{\theta}$, $\hat{\psi}$, $\hat{p}$, $\hat{q}$, $\hat{r}$, $\hat{h}$, $\hat{V}_a$) as compared to the directly measured variables. An example output of these measures is shown in Fig. A.4. The mean difference, the variance about this mean, and the resultant standard deviation are computed for the entire length of the run. The first three variables are the roll, pitch, and yaw estimates compared to the INS measurements. The second three variables (nos. 4, 5, and 6) are the roll, pitch, and yaw rate estimates compared to the rate gyro measurements. The seventh line compares the smoothed altitude to the barometric altimeter measurements. The eighth line compares the smoothed airspeed to the J-Tek true airspeed measurement.

A third option of the program (using Option Flag NF8) is to produce computer generated plots of the estimated and measured attitude angles and rates. An example plot of the roll angle is shown in Fig. A.5. In this plot, the asterisk (*) represents the INS measurement of roll angle ϕ. The 0 is the estimated roll angle $\hat{\phi}$. The plus sign (+) is the difference which is used to compute the statistical measures. These plots are automatically scaled so that the width of the entire page is used.

A fourth option of the program (using Option Flag NF9) is to produce plots from the Ames Zeta plotter. This option writes a data set, and the plot is produced by use of a different program. An example of this type of plot is shown in Fig. A.6.

Program Explanation

Overview.- An overview of the ESTEST program is represented by the block diagram in Fig. A.7. After the initialization calculations have been made and the data set has been advanced to the desired starting point, the program enters an iterative loop It remains in this loop until the last desired

59

T	FI FIH FIM GYH HHH	THET THTH TNT4 GYH BHP	ST STH STM GZH RHC	P PH PDM GAM BHR	Q QH UDM QH	R RH RDM AMN	FX H BX BXH	FY HH BY BYH	FZ ALH BZ BZH	VI VAH KHD FL
7.022E-02	-4.196E 00 -4.196E 00	-1.582E 00 -1.582E 00	1.311E 02 1.311E 02	2.064E 00 2.064E 00	8.341E-01 8.341E-01	1.714E 00 1.714E 00	1.564E 00 1.950E 03	-7.281E-01 1.950E 03	-3.490E 01 -1.582E 00	1.904E 02 1.904E 02
1.404E-01	-4.350E 00 -3.865E 00 9.667E 00 8.879E-01 0.000	-1.494E 00 -1.494E 00 0.000 -2.353E 00 7.788E-03	1.314E 02 1.301E 02 1.178E 02 3.207E 01 0.000	-1.496E 00 -1.810E 00 2.270E 00 -8.828E 00 -1.810E-02	8.341E-01 8.341E-01 0.000 4.071E 01	1.656E 00 1.479E 00 -2.312E-01 0.000	1.722E 00 1.947E 03 -9.374E 01 0.000	-9.855E-01 1.947E 03 -2.531E 02 0.000	-3.512E 01 0.000 3.891E 02 0.000	2.042E 02 1.904E 02 -2.922E 01 -6.387E-01
2.107E-01	-4.504E 00 -3.569E 00 8.363E 00 8.879E-01 -1.705E-03	-1.450E 00 -1.450E 00 0.000 -2.353E 00 1.466E-02	1.315E 02 1.291E 02 1.163E 02 3.207E 01 0.000	-1.042E 00 -1.484E 00 3.449E 00 -8.751E 00 -3.651E-02	9.471E-01 8.658E-01 4.521E-01 4.092E 01	1.714E 00 1.259E 00 6.493E-02 0.000	1.999E 00 1.942E 03 -9.140E 01 0.000	-6.178E-01 1.945E 03 -2.672E 02 0.000	-3.334E 01 0.000 4.055E 02 0.000	2.047E 02 1.909E 02 -2.904E 01 -4.018E-01
2.809E-01	-4.592E 00 -3.304E 00 7.119E 00 8.879E-01 -8.492E-03	-1.362E 00 -1.362E 00 0.000 -2.353E 00 2.066E-02	1.316E 02 1.281E 02 1.171E 02 3.207E 01 0.000	-1.042E 00 -1.236E 00 2.480E 00 -8.723E 00 -5.380E-02	4.385E-01 7.458E-01 -1.709E 00 4.113E 01	1.656E 00 1.033E 00 -1.845E-01 0.000	2.117E 00 1.938E 03 -9.374E 01 0.000	-1.096E 00 1.943E 03 -2.508E 02 0.000	-3.312E 01 0.000 4.031E 02 0.000	1.941E 02 1.918E 02 -2.903E 01 -8.757E-01
3.511E-01	-4.680E 00 -3.073E 00 5.864E 00 8.879E-01 -1.450E-02	-1.274E 00 -1.274E 00 0.000 -2.353E 00 2.501E-02	1.318E 02 1.272E 02 1.175E 02 3.207E 01 0.000	-8.719E-01 -9.994E-01 2.465E 00 -8.729E 00 -7.050E-02	4.385E-01 6.595E-01 -1.229E 00 4.117E 01	1.540E 00 7.863E-01 -5.950E-01 0.000	2.236E 00 1.934E 03 -9.608E 01 0.000	-1.721E 00 1.941E 03 -2.508E 02 0.000	-2.933E 01 0.000 4.031E 02 0.000	2.084E 02 1.915E 02 -2.906E 01 -6.387E-01
4.213E-01	-4.790E 00 -2.865E 00 4.069E 00 6.879E-01 -1.395E-02	-1.230E 00 -1.230E 00 0.000 -2.353E 00 3.005E-02	1.319E 02 1.263E 02 1.185E 02 3.207E 01 0.000	-1.156E 00 -9.016E-01 6.371E-01 -8.800E 00 -8.606E-02	6.080E-01 6.450E-01 -2.058E-01 4.143E 01	1.425E 00 5.305E-01 -8.902E-01 0.000	1.722E 00 1.942E 03 -9.843E 01 0.000	-1.464E 00 1.938E 03 -2.227E 02 0.000	-3.445E 01 0.000 4.031E 02 0.000	1.936E 02 1.921E 02 -7.939E 01 -4.018E-01

FIGURE A.3.- OUTPUT DATA HEADER AND SAMPLE NUMERICAL DATA

TABLE A.4.- DEFINITION OF ACRONYMS IN DATA HEADER OF
FIGURE A.3

LINE	ACRONYM	EXPLANATION
1	T	Time from beginning of run (sec)
	FI	Roll angle from INS (deg)
	THET	Pitch angle from INS (deg)
	SI	Heading (or yaw) angle from INS (or directional gyro) (deg)
	P	Rate gyro measured roll rate (deg/sec)
	Q	Rate gyro measured pitch rate (deg/sec)
	R	Rate gyro measured yaw rate (deg/sec)
	FX	Longitudinal acceleration (ft/sec^2 or g's)
	FY	Lateral acceleration (ft/sec^2 or g's)
	FZ	Vertical acceleration (ft/sec^2 or g's)
	VI	J-Tek measured true airspeed (ft/sec)
2	FIH	Estimated roll angle (deg)
	THTH	Estimated pitch angle (deg)
	SIH	Estimated yaw angle (deg)
	PH	Estimated roll rate (deg/sec)
	QH	Estimated pitch rate (deg/sec)
	RH	Estimated yaw rate (deg/sec)
	H	Barometric altitude (ft)
	HH	Smoothed altitude (ft)
	ALH	Estimated angle-of-attack (deg)
	VAH	Smoothed true airspeed (ft/sec)

TABLE A.4 (Continued)

LINE	ACRONYM	EXPLANATION
3	FIM —	Roll-angle determined from magnetometer data (deg)
	THIM	Pitch angle determined from magnetometer or accelerometer and dynamic pressure data (deg)
	SIM	Yaw angle determined from magnetometer data (deg)
	PDM	Derived roll acceleration (deg/sec^2)
	QDM	Derived pitch acceleration (deg/sec^2)
	RDM	Derived yaw acceleration (deg/sec^2)
	BX	Measured or derived longitudinal component of magnetic field
	BY	Measured or derived lateral component of magnetic field
	BZ	Measured or derived vertical component of magnetic field
	HHD	Estimated altitude rate (ft/sec)
4	GXH	Estimated longitudinal component of gravity (ft/sec^2)
	GYH	Estimated lateral component of gravity (ft/sec^2)
	GZH	Estimated vertical component of gravity (ft/sec^2)
	GAM	Flight path angle (deg)
	QH	Derived dynamic pressure (lb/ft^2)
	AMN	Measured angle-of-attack as function of dynamic pressure, vertical acceleration, and flap angle (deg)
	BXH	Smoothed longitudinal component of magnetic field
	BYH	Smoothed lateral component of magnetic field
	BZH	Smoothed vertical component of magnetic field

LINE	ACRONYM	EXPLANATION
4	FL	Flap angle (deg)
5	BHH	Estimated acceleration bias in altitude filter (ft/sec^2)
	BHP	Estimated acceleration bias in roll filter (deg/sec^2)
	BHQ	Estimated acceleration bias in pitch filter (deg/sec^2)
	BHR	Estimated acceleration bias in yaw filter (deg/sec^2)

STATISTICAL PERFORMANCE MEASURES

```
NO : 1   MEAN: 5.55333E-01   VARIANCE: 1.95178E-01   STD DEV: 4.41789E-01
NO : 2   MEAN:    0.00000    VARIANCE:    0.00000    STD DEV:    0.00000
NO : 3   MEAN:-9.98562E-01   VARIANCE: 2.20264E 00   STD DEV: 1.48413E 00
NO : 4   MEAN: 1.51040E-01   VARIANCE: 6.40981F-01   STD DEV: 8.00613E-01
NO : 5   MEAN:-6.23727E-02   VARIANCE: 6.03886E-02   STD DEV: 2.45741E-01
NO : 6   MEAN:-1.39423E-01   VARIANCE: 4.61311E-01   STD DEV: 6.79199E-01
NO : 7   MEAN: 1.12500E-02   VARIANCE: 3.04831E 01   STD DEV: 5.52115E 00
NO : 8   MEAN: 6.21155F 00   VARIANCE: 7.16098E 01   STD DEV: 8.46226E 00
```

FIGURE A.4.- EXAMPLE PROGRAM STATISTICAL PERFORMANCE MEASURES

CHART 1

TIME - SEC

FIGURE A.5.– EXAMPLE OF THE COMPUTER GENERATED
ESTIMATE PLOT

65

FIGURE A.5.- (CONTINUED)
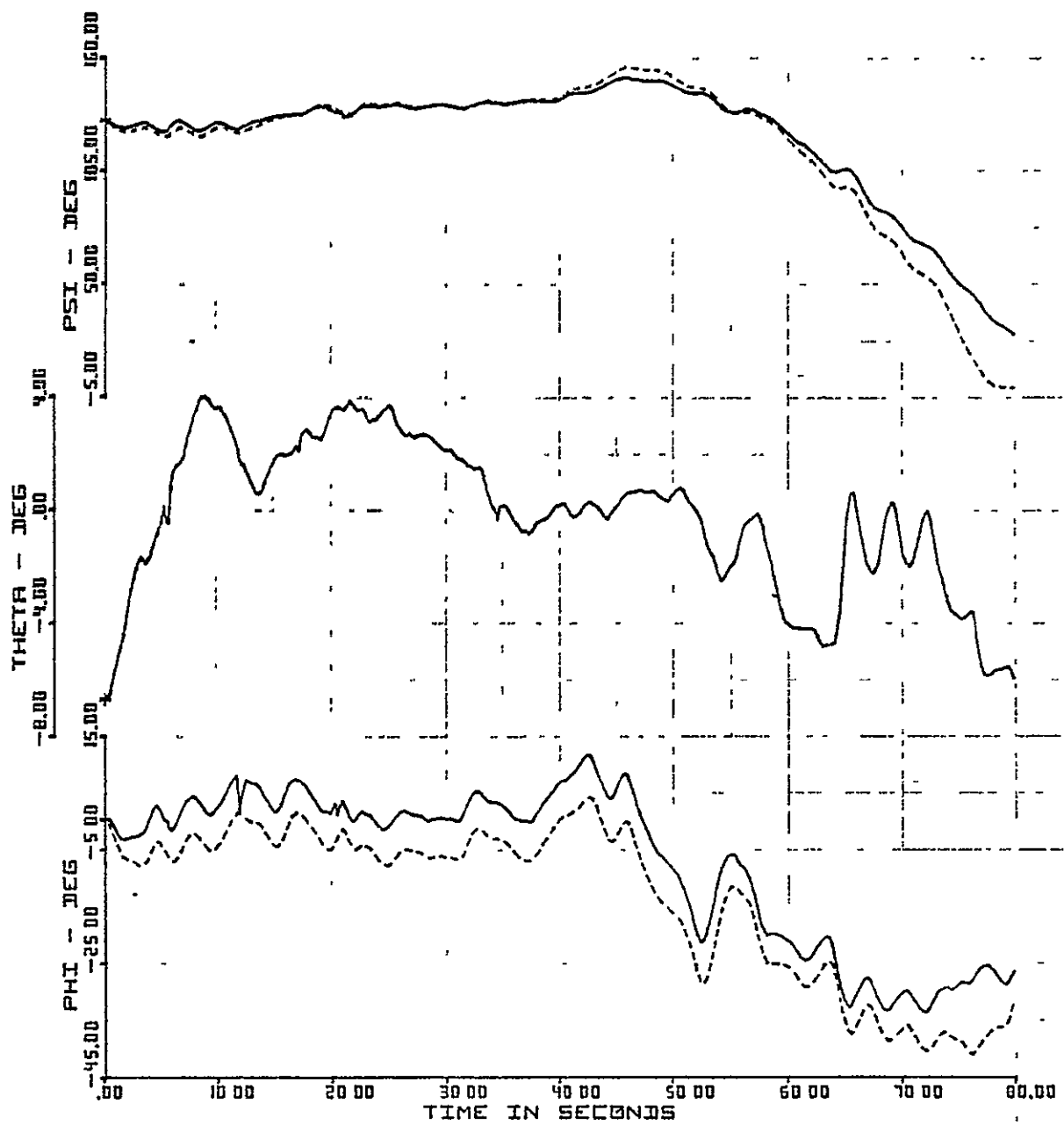
TIME - SEC

ROLL ANGLE - DEG

66
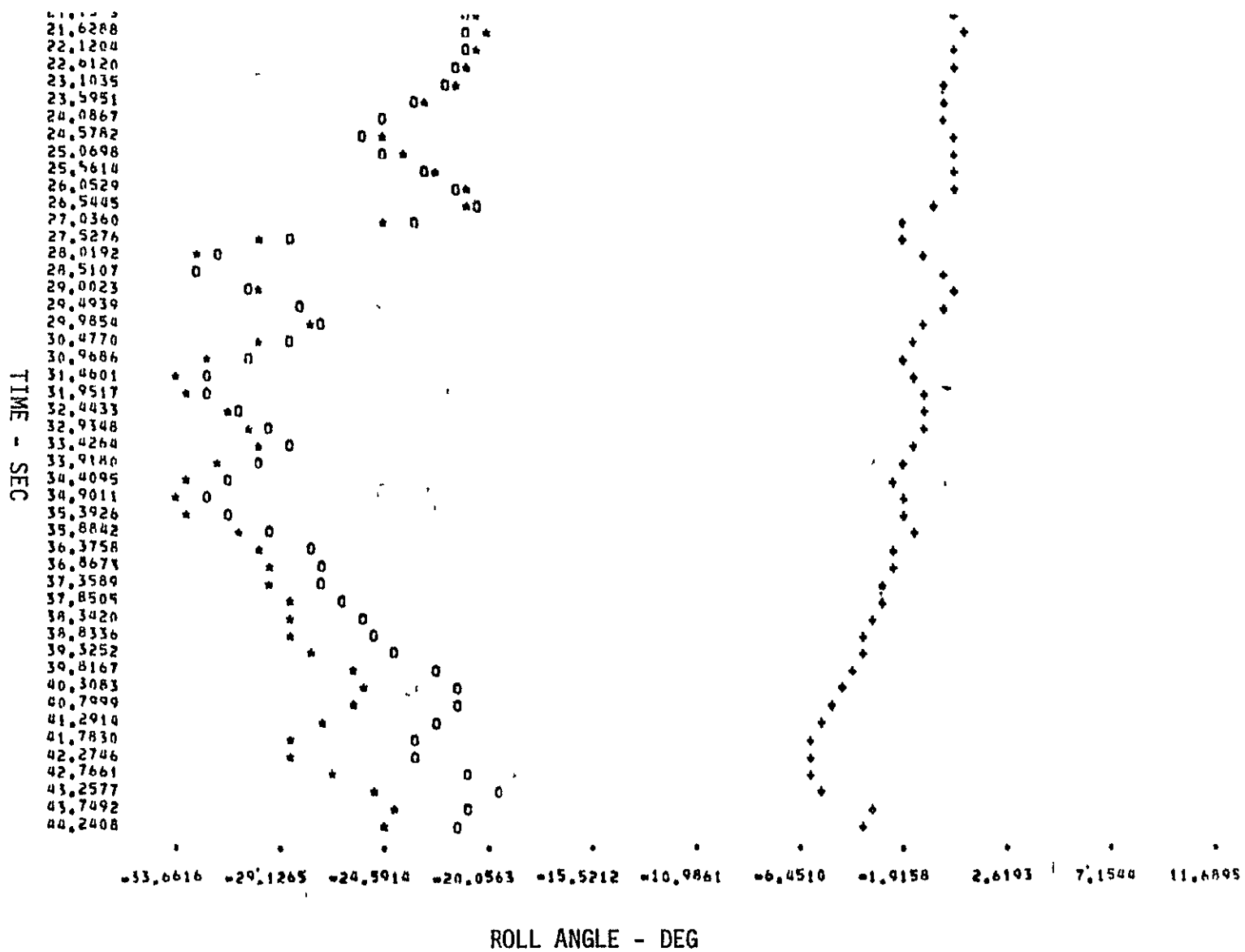
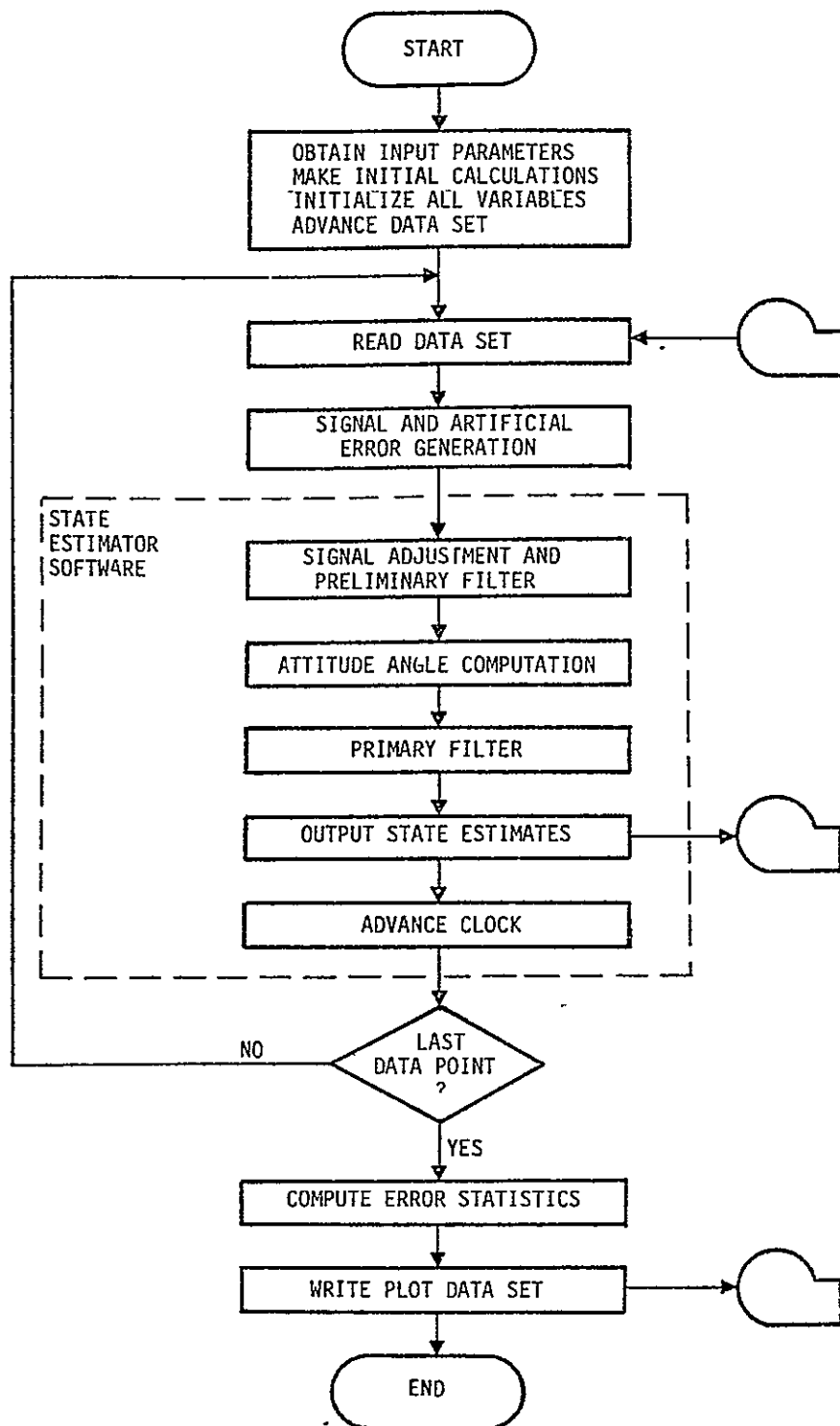FIGURE A.6.- EXAMPLE OF ZETA PLOTTER OUTPUT

FIGURE A.7.- PROGRAM FLOW CHART

data point has been processed. Reading the data is similar to taking sampled measurements from the on board sensors.

Following the reading of the data, the option is available to add artificial errors to these data. This allows the user to investigate, for any data sequence, the effect of the errors on the estimation accuracy. In this way, the sensor accuracy can be specified.

In addition to adding artificial errors, artificial sensor signals may also be generated. For example, for the CV-990 data, artificial magnetometer readings were generated as a function of the INS and directional gyro mreasurements of (φ, θ, ψ).

After the sampled measurement signals are prepared, the program enters a block which represents a replica of the digital state estimator which would be implemented on board the aircraft. This has five steps, as indicated in Fig. A.7. The signal adjustment, attitude angle, and primary filter computations are discussed in detail in Chapter II. Outputting the state estimates is analogous to using the estimates for cockpit display or to drive a flight director or autopilot.

When the final data point has been processed, the statistical measures presented in Fig. A.4 are computed. Also, the resulting plots, such as shown in Figs. A.5 and A.6, are prepared.

Artificial signal generation.- There are four sets of measurements which may be required to be generated artificially from other sensor readings. These include the magnetic field, the angular acceleration, the true airspeed, and the dynamic pressure.

Generation of the three components of the magnetic field requires knowledge of the vector magnitude B_{mag} and the dip angle δ_2. Then the magnetic north and downward components of the field are, respectively,

$$B_{xo} = B_{mag} \cos \delta_2 \quad ,$$

$$B_{zo} = B_{mag} \sin \delta_2 \quad . \tag{A.1}$$

From the INS (and possibly the directional gyro), the roll, pitch, and yaw angles (φ, θ, ψ) of the aircraft are read. From these, the three body-fixed components of the magnetic field are computed to be

$$B_x = B_{xo} \cos \theta \cos \psi - B_{zo} \sin \theta,$$

$$B_y = B_{xo}(\sin \varphi \sin \theta \cos \psi - \cos \varphi \sin \psi)$$

$$+ B_{zo} \sin \varphi \cos \theta,$$

$$B_z = B_{xo}(\cos \varphi \sin \theta \cos \psi + \sin \varphi \sin \psi)$$

$$+ B_{zo} \cos \varphi \cos \theta. \tag{A.2}$$

The rate gyro measurements (p, q, r) are used to generate artificial angular accelerometer data. For the Cessna 402B data where unsmoothed gyro samples were taken approximately every 0.07 sec, the samples were first smoothed using a simple lag filter, e.g.,

$$\dot{p}_f = k_{B1}(p - p_f) \tag{A.3}$$

Here, p_f is the smoothed value of the measured roll rate p, and k_{B1} is the inverse time constant of the filter. This is implemented digitally as

$$p_{f+1} = k_{B1} \Delta t (p_{n+1} - p_f) + p_f . \tag{A.4}$$

Here, p_{n+1} is the measured rate at the n+1 time point. Also, p_f and p_{f+1} indicate the filtered rates at the time points n and n+1. Then, the artificial angular acceleration is computed as a simple difference; e.g.,

$$\dot{p} = (p_{f+1} - p_f)/\Delta t . \tag{A.5}$$

In Eqs. (A.4) and (A.5), Δt is the sample time. For the CV-990 data, where 20 samples were added and averaged to produce data points approximately 1 sec apart, Eq. (A.5) was used directly without first filtering.

If pitot tube measurements are used, conversion is necessary from indicated (V_m) to true airspeed (V_a). Incompressible flow is assumed, so that

$$V_a = V_m \sqrt{\rho_o/\rho} \triangleq V_m S. \tag{A.6}$$

70

The quantity S $(= 1/\sqrt{\sigma} = \sqrt{\rho_o/\rho})$ is computed using linear interpolation from a table with quantities as a function of smoothed altitude $\hat{h}$. The interpolation equation is

$$S = S_L + \frac{(S_H - S_L)}{(h_H - h_L)} (\hat{h} - h_L) ,$$

$$\triangleq S_L + S_{oh}(\hat{h} - h_L) . \qquad (A.7)$$

The quantities S_L, S_{oh}, and h_L are presented in Table 5.

If dynamic pressure (Q) measurements are required, they are generated from the smoothed true airspeed using the equation

$$\hat{Q} = 0.001189 \, \sigma \, \hat{V}_a^2 \qquad (A.8)$$

Here, the quantity σ again comes from linear interpolation as a function of altitude:

$$\sigma = \sigma_L + \sigma_{oh}(\hat{h} - h_L) . \qquad (A.9)$$

The quantities σ_L and σ_{oh} also appear in Table A.5. This table and Eqs. (A.6)-(A.9) appear in subroutines CONV and CONV1.

TABLE A.5.- TABLE LOOKUP QUANTITIES USED TO COMPUTE TRUE
AIRSPEED AND DYNAMIC PRESSURE

ALTITUDE h_L, FT	DENSITY RATIO S_L	S_{oh}, 1/FT x 10^5	DENSITY RATIO σ_L	σ_{oh}, 1/FT x 10^4
0	1.0		1.0	
2000	1.02991	1.4955	0.94277	-0.28615
5000	1.07728	1.5790	0.86167	-0.27033
10000	1.16367	1.7278	0.73848	-0.24638

Artificial error generation - The option flag NF3 is used to indicate whether artificial errors are added to the signal measurements.

For the magnetometer readings, the signals (B_x, B_y, B_z) are subject to sensor misalignment angles $(\varphi_B, \theta_B, \psi_B)$, triad skew angles $(\psi_{By}, \theta_{Bz}, \varphi_{Bz})$, biases (b_{Bx}, b_{By}, b_{Bz}), scale factor errors $(\varepsilon_{Bx}, \varepsilon_{By}, \varepsilon_{Bz})$, and noise terms $(\eta_{Bx}, \eta_{By}, \eta_{Bz})$. The equations which introduce these errors are:

$$B'_{xm} = B_x + \psi_B B_y - \theta_B B_z \ ,$$

$$B'_{ym} = -\psi_B B_x + B_y + \varphi_B B_z \ ,$$

$$B'_{zm} = \theta_B B_x - \varphi_B B_y + B_z \ ,$$

$$B''_{xm} = B'_{xm} \ ,$$

$$B''_{ym} = -\psi_{By} B'_{xm} + B'_{ym} \ ,$$

$$B''_{zm} = \theta_{Bz} B'_{xm} - \varphi_{Bz} B'_{ym} + B'_{zm} \ ,$$

$$B_{xm} = (1 + \varepsilon_{Bx}) B''_{xm} + b_{Bx} + \eta_{Bx} \ ,$$

$$B_{ym} = (1 + \varepsilon_{By}) B''_{ym} + b_{By} + \eta_{By} \ ,$$

$$B_{zm} = (1 + \varepsilon_{Bz}) B''_{zm} + b_{Bz} + \eta_{Bz} \ . \tag{A.10}$$

The noise terms $(\eta_{Bx}, \eta_{By}, \eta_{Bz})$ are generated each sample point by using a random number generator with assumed Gaussian statistics and standard deviations $(\sigma_{Bx}, \sigma_{By}, \sigma_{Bz})$. Other noise terms subsequently mentioned are generated in a similar manner.

The angular accelerometer signals $(\dot{p}_n, \dot{q}_n, \dot{r}_n)$ are subject to misalignment angles $(\varphi_{\dot{p}}, \theta_{\dot{p}}, \psi_{\dot{p}})$, scale factor errors $(\varepsilon_{\dot{p}}, \varepsilon_{\dot{q}}, \varepsilon_{\dot{r}})$, biases $(b_{\dot{p}}, b_{\dot{q}}, b_{\dot{r}})$, and noise terms $(\varepsilon_{\dot{p}}, \varepsilon_{\dot{q}}, \varepsilon_{\dot{r}})$. These are introduced as

$$\dot{p}_m = (1 + \varepsilon_{\dot{p}})(\dot{p}_n + \psi_{\dot{p}}\dot{q}_n - \theta_{\dot{p}}\dot{r}_n) + b_{\dot{p}} + \eta_{\dot{p}} \ ,$$

$$\dot{q}_m = (1 + \varepsilon_{\dot{q}})(-\psi_{\dot{p}}\dot{p}_n + \dot{q}_n + \varphi_{\dot{p}}\dot{r}_n) + b_{\dot{q}} + \eta_{\dot{q}} \ ,$$

$$\dot{r}_m = (1 + \varepsilon_{\dot{r}})(\theta_{\dot{p}}\dot{p}_n - \varphi_{\dot{p}}\dot{q}_n + \dot{r}_n) + b_{\dot{r}} + \eta_{\dot{r}} \ . \qquad (A.11)$$

The linear accelerometer signals (f_x, f_y, f_z) are subject to position errors with respect to the aircraft center of gravity (x_a, y_a, z_a), misalignment angles $(\varphi_a, \theta_a, \psi_a)$, scale factor errors $(\varepsilon_{ax}, \varepsilon_{ay}, \varepsilon_{az})$, biases (b_{ax}, b_{ay}, b_{az}), and noise terms $(\eta_{ax}, \eta_{ay}, \eta_{az})$. The error equations are

$$f'_x = \dot{q}_n z_a - \dot{r}_n y_a - (q_n^2 + r_n^2)x_a + p_n(q_n y_a + r_n z_a) + f_x \ ,$$

$$f'_y = \dot{r}_n x_a - \dot{p}_n z_a - (p_n^2 + r_n^2)y_a + q_n(p_n x_a + r_n z_a) + f_y \ ,$$

$$f'_z = \dot{p}_n y_a - \dot{q}_n x_a - (p_n^2 + q_n^2)z_a + r_n(p_n x_a + q_n y_a) + f_z \ ,$$

$$f_{xm} = (1 + \varepsilon_{ax})(f'_x + \psi_a f'_y - \theta_a f'_z) + b_{ax} + \eta_{ax} \ ,$$

$$f_{ym} = (1 + \varepsilon_{ay})(-\psi_a f'_x + f'_y + \varphi_a f'_z) + b_{ay} + \eta_{ay} \ ,$$

$$f_{zm} = (1 + \varepsilon_{az})(\theta_a f'_x - \varphi_a f'_y + f'_z) + b_{az} + \eta_{az} \ . \qquad (A.12)$$

The airspeed measurement V_a is subject to scale factor error ε_v, bias b_v, and noise η_v, as

$$V_{am} = (1 + \varepsilon_v)V_a + b_v + \eta_v \qquad (A.13)$$

The barometric altimeter measurement is similarly affected by scale factor error ε_h, bias b_h, and noise η_h

$$h_m = (1 + \varepsilon_h)h_b + b_h + \eta_h \qquad (A.14)$$

Estimate mean and standard deviation.- Let $\Delta\varphi_n$ be the difference between the estimated roll angle $\hat{\varphi}$ and the measured roll angle φ at the nth sample point of a sequence of m points Then, the mean difference in $\hat{\varphi}$ is

73

$$\overline{\Delta\varphi} \triangleq E\{\Delta\varphi\} = \frac{1}{m} \sum_{n=1}^{m} \Delta\varphi_n \quad . \tag{A.15}$$

The sample variance about the mean is

$$\sigma^2_{\Delta\varphi} \triangleq E\{\Delta\varphi^2\} = \frac{1}{m-1} \sum_{n=1}^{m} (\Delta\varphi_n - \overline{\Delta\varphi})^2 \tag{A.16}$$

This is computed by storing the residuals $\Delta\varphi_n$ as $\overline{\Delta\varphi}$ is computed in Eq. (A.15). Then, Eq. (A.16) is computed on a second pass through the data.

Similar means and variances are computed for $\hat{\theta}$, $\hat{\psi}$, $\hat{p}$, $\hat{q}$, $\hat{r}$, $\hat{V}_a$, and $\hat{h}$. These do not represent absolute errors in the estimates. Rather, they represent the statistical differences between the estimated and directly measured quantities. The INS and rate gyro measurements are also subject to errors, and these errors are included in the statistics. However, because the INS and rate gyro measurements are considered to be of extremely high quality with regard to flight control applications, they serve as a reasonable standard with which to assess the estimators.

APPENDIX B

METHOD NO. 2 STATE ESTIMATOR SOFTWARE

Chapter IV presents preliminary estimates of the requirements to mechanize the Method No. 2 state estimator on a typical microcomputer in terms of memory and run times. To make these estimates required definition of specific estimator software and coding on a PDP 11 computer. This appendix presents the Method 2 estimator code in FORTRAN form. Input variables, program constants, and initial computations are also given. Then, a listing of the main estimator cycle computations in C language (UNIX system) for the PDP 11 is presented.

Method No. 2 Mechanization

Computer arithmatic, logic, and function requirements.-

+	add
-	subtract
*	multiply
/	divide
SQRT	square root
SIN	sine
CØS	cosine
ARSIN	arc sine
ARCØS	arc cosine
ABS	absolute value
.GT.	greater than
.LT.	less than
.AND.	logical AND
IF, THEN	
GØ TØ	labeled GØ TØ

Definition of constants and program variables.-

Constants used throughout program·

ØPXC,ØPYC,ØPZC
BAXC,BAYC,BAZC } Correction terms for linear accelerometer
SAMR,TAMR,FAMR

RKUT - Airspeed smoothing gain

HL(1),HL(2),HL(3)
SØH(1),SØH(2),SØH(3) } Table quantities to compute $\hat{Q}$
SL(1),SL(2),SL(3)
CØN1

Constants used throughout program (Cont'd):

SALR,TALR,FALR - Correction terms for angular
                  accelerometer

OCBX,OCBY,OCBZ ⎞
BCBX,BCBY,BCBZ ⎬ Correction terms
SCXR,TCXR,SCYR,FCYR,TCZR,FCZR ⎠ for magnetometer

ALR$\emptyset$,ALR1,ACN - (ACN function of aircraft mass)
BX$\emptyset$,BZ$\emptyset$ - (Function of local magnetic field)
DT,DTT,DTQ - Δt, $\Delta t^2/2$, $\Delta t^3/6$
TPI,TP$\emptyset$T,P$\emptyset$T - 2π, $3\pi/2$, $\pi/2$
H$\emptyset$,G - (H$\emptyset$ function of local barometric pressure)
RKBH,RK1,RK2 ⎞
RKBP,RK3,RK4 ⎟
RKBQ,RK5,RK6 ⎬ Primary filter gains
RKBR,RK7,RK8 ⎠

Variables initialized to zero or known values:

BHHN,HHD   - Altitude bias and rate
BHPN,PHN,FIHN   - Roll accelerometer bias, roll
                  rate, and angle
BHQN,QHN,ALHN   - Pitch accelerometer bias and
                  pitch rate, and angle-of-attack
BHRN,RHN   - Yaw accelerometer bias and yaw
                  rate
VAH   - True airspeed

Variables initialized by direct reading or input:

HHN=HM   - Altitude
DL2   - Local magnetic field dip angle
RM   - Aircraft average mass
T   - Time

Variables initialized by computation:

BX$\emptyset$=C$\emptyset$S(DL2) ⎞ Local North and down components
BZ$\emptyset$=SIN(DL2) ⎠ of magnetic field
ACN=RM/(CZAL*SW) - (CZAL: stored lift coeffi-
                    cient, SW: reference wing
                    area)

Measured (sampled) input variables:

FXM,FYM,FZM - linear accelerometer
VM   - true airspeed
PDM,QDM,RDM - angular accelerometer
BXM,BYM,BZM - magnetic field
HM   - barometric altitude
FLPR   - flap angle

Initial computation to obtain initial yaw angle (on ground).-

(1)   Measure BXM,BYM from magnetometer

(2)   Use equations (given later) to remove magnetometer errors and normalize BXM,BYM to BUX,BUY.

(3)   Compute:

```
BMB=1./SQRT(BUX*BUX+BUY*BUY)
CSI=BUX*BMB
SSI=-BUY*BMB
SIHN=ARCØS(CSI)
IF(SSI.LT.0.)SIHN=TPI-SIHN.
```

Computations of main estimator equations (cyclic).-

(1)   Read sampled input variables from buffers.

(2)   Modification of sensor readings.

Remove linear accelerometer scale factor error, bias, and misalignment:

```
FXM=ØPXC*FXM+BAXC
FYM=ØPYC*FYM+BAYC
FZM=ØPZC*FAM+BAZC
FXN=FXM+SAMR*FYM-TAMR*FZM
FYN=-SAMR*FXM+FYM+FAMR*FZM
FZN=TAMR*FXM-FAMR*FYM+FZM
```

Smooth true airspeed and compute $\hat{Q}$

```
VAH=VAH+RKUT*(VM-VAH)
I=1
IF(HNN.GT.HL(2))I=2
IF(HHN.GT.HL(3))I=3
SIG=SL(I)+SØH(I)*(HHN-HL(I))
QH=CØN1*SIG*VAH*VAH
```

Remove angular accelerometer misalignment:

```
PDN=PDM+SALR*QDM-TALR*RDM
QDN=-SALR*PDM+QDM+FALR*RDM
RDN=TALR*PDM-FALR*QDM+RDM
```

77

Remove magnetometer scale factor error, bias, and misalignment. Normalize.

```
BXM=ØCBX*BXM+BCBX
BYM=ØCBY*BYM+BCBY
BZM=ØCBZ*BZM+BCBZ
BXN=BXM+SCXR*BYM+TCXR*BZM
BYN=BYM+SCYR*BXM+FCYR*BZM
BZN=BZM+TCZR*BXM+FCZR*BYM
ØBMAG=1./SQRT(BXN*BXN+BYN*BYN+BZN*BZN)
BUX=BXN*ØBMAG
BUY=BYN*ØBMAG
BUZ=BZN*ØBMAG
```

(3) <u>Compute independent angles.</u>

Angle-of-attack, flight path angle, and pitch angle·

```
ALZR=ALRØ+ALR1*FLPR
AMN=ALZR-ACN*FZN/QH
SGAM=HHD/VAH
GAMP=ARSIN(SGAM)
THHN=GAMP+ALHN*CØS(FIHN)
```

Roll and yaw angles·

```
STHH=SIN(THHN)
CTHH=CØS(THHN)
CSIM=(BUX+BZØ*STHH)/(BXØ*CTHH)
TA=(BUZ*BUZ+BUY*BUY)*CTHH*CTHH
TB=-2.*(BZØ+BUX*STHH)*BUZ*CTHH
TC1=(BZØ+BUX*STHH)*(BZØ+BUX*STHH)
TC=TC1-BUY*BUY*CTHH*CTHH
DIS=TB*TB-4.*TA*TC
DISR=SQRT(DIS)
CFMI=0.5*(-TB+DISR)/TA
CFM2=0.5*(-TB-DISR)/TA
SFM1=BUY*(CFM1*CFM1-1.)/(BUZ*CFM1-BZØ+CTHH
      -BXØ*STHH*CSIM)
SFM2=BUY*(CFM2*CFM2-1.)/(BUZ*CFM2-BZØ*CTHH
      -BXØ*STHH*CSIM)
FMPLS=FIM+PHN*DT
SNMØ=SIN(FMPLS)
DSF1=ABS(SFM1-SNMØ)
DSF2=ABS(SFM2-SNMØ)
IF(DSF2 LT.DSF1) GØ TØ 10
CFM=CFM1
SFM=SFM1
GØ TØ 20
10  CONTINUE
CFM=CFM2
SFM=SFM2
```

Roll and yaw angles (Cont'd):

```
20   CONTINUE
     FIM=ARSIN(SFM)
     SSIM=(SFM-BUY*CFM/BUZ)*BUZ/BXØ
     SIM=ARCØS(CSIM)
     IF(SSIM.LT.0.)SIM=TPI-SIM
```

(4) <u>Primary filter</u>.

Preliminary computations:

```
IF((SIM.GT.TPØT).AND.(SIHN.LT.PØT))SIHN=SIHN+TPI
IF((SIM.LT.PØT).AND.(SIHN.GT.TPØT))SIHN=SIHN-TPI
RSI=SIM-SIHN
RFI=FIM-FIHN
RAL=AMN-ALHN
RH=HM+HØ-HHN
SFIH=SIN(FIHN)
CFIH=CØS(FIHN)
TTHH=STHH/CTHH
C0=RKBH*RH
C1=FXN*STHH-FYN*SFIH*CTHH-FZN*CFIH*CTHH-G
    +RK1*RH+BHHN
C2=RK2*RH
CBP=RKBP*RFI
C3=PDN+RK3*RFI+BHPN
C4=RK4*RFI
CCP=RKBQ*RAL
C5=QDN+RK5*RAL+BHQN
C6=RK6*RAL+(FZN+G*CFIH*CTHH)/VAH
CDP=RKBR*CFIH*CTHH*RSI
C7=RDN+RK7*CFIH*CTHH*RSI+BHRN
C8=RK8*RSI
```

Altitude filter

```
BHHP=BHHN+C0*DT
HHDP=HHD+C1*DT+C0*DTT
HHP=HHN+(HHD+C2)*DT+C1*DTT+C0*DTQ
```

Roll filter·

```
BHPP=BHPN+CBP*DT
PHNP=PHN+C3*DT+CBP*DTT
FIHP=FIHN+(PHN+(QHN*SFIH+RHN*CFIH)*TTHH+CR)*DT
     +(C3+(C5*SFIH+C7*CFIH)*TTHH)*DTT
     +(CBP+(CCP*SFIH+CDP*CFIH)*TTHH)DTQ
```

Angle-of-attack filter:

```
BHQP=BHQN+CCP*DT
QHNP=QHN+C5*DT+CCP*DTT
ALHP=ALHN+(QHN+C6)*DT+C5*DTT+CCP*DTQ
```

Yaw filter:

```
BHRP=BHRN+CDP*DT
RHNP=RHN+C7*DT+CDP*DTT
SIHP=SIHN+C8*DT+((RHN*CFIH+QHN*SFIH)*DT
      +(C7*CFIH+C5*SFIH)*DTT)/CTHH
      +(CDP*CFIH+CCP*SFIH)*DTQ/CTHH
```

Time update:

```
T=T+DT
BHHN=BHHP
HHD=HHDP
HHN=HHP
BHPN=BHPP
BHQN=BHQP
BHRN=BHRP
PHN=PHNP
QHN=QHNP
RHN=RHNP
FIHN=FIHP
ALHN=ALHP
SIHN=SIHP
```

(5) <u>Output estimates (display and/or control computations).</u>

(6) <u>Cycle back to read new samples.</u>

Main Estimator Code in UNIX C Language

```
main(){
float fxm,fym,fzm,opxc,opyc,opzc,baxc,bayc,bazc,rkbh,
fxn,fyn,fzn,samr,tamr,tamr,van,rkut,vm,hhn,
hl[3],sl[3],soh[3],sig,gh,con1,pdn,qdn,rdn,
pdm,qdm,rdm,salr,talr,falr,bxm,bym,bzm,
ocbx,ocbv,ocoz,ocby,rcby,ncbz,bxn,byn,bzn,
scxr,scyr,tcxr,tczr,fcvr,fczr,obmag,
bux,buy,buz,alzr,alro,alr1,flpr,amn,acn,
soam,hhd,qamp,thnn,alhn,fihn,stnh,cthh,
bxo,bzo,csim,ta,tp,tc,dis,disr,cfm1,cfm2,
sfm1,sfm2,tmpls,pnp,ot,snmo,dsf1,dsf2,
cfm,sfm,fin,ssin,sin,tpi,tpot,pot,sihn,rsi,
rfi,ral,rh,am,ho,nnn,stih,cfih,tthh,c0,c1,g,
rki,bnhn,c2,rk2,cbp,rkbp,c3,rk3,bhpn,
c4,rk4,ccp,rkbq,c5,rk5,bhqn,c6,rk6,cdp,
rkbr,c7,rk7,ohrn,c8,rk8,bnnp,hhdp,dtt,
hhp,atq,pnpp,phnp,fihp,ohn,rhn,bhqp,qhnp,
alhp,bnrp,rnnp,sihp,t;
int i;
```

```
read:
fxm = opxc*fxm + paxc;
fym = opyc*fym + payc;
fzm = opzc*tzm + pazc;
fxn = fxm + samr*fym - tamr*fzm;
fyn = -samr*fxm + fym + famr*fzm;
fzn = tamr*fxm - famr*fym + fzm;
van = vah + rkuf*(vm - van);
1 = 0;
if (nnn > nl[1]) 1 = 1;
if (nhn > nl[2]) 1 = 2;
sig = sl[1] + snpf[1]*(nnn - hl[1]);
qh = conl*sig*(pow(van,2));
pnn = pdm + sqlr*rdm - talr*rdm;
qdn = -sqlr*pdm + qdp + falr*rom;
rdn = talr*pda - falr*odm + rom;
bxn = ocpx*bxm + ocpx;
byn = ocpy*bym + ocpy;
bzn = ocpz*bzm + hcpz;
bxn = bxm + scxr*bym + tcxr*bzm;
byn = bym + scyr*bxm + fcyr*bzm;
bzn = bzm + tczr*bxm + fczr*bym;
obmag = 1/sqrt(bxn*bxn + byn*byn + bzn * bzn);
bux = bxn*obmag;
buy = byn*obmag;
buz = bzn*obmag;


alzr = alro + alrl*flpr;
amn = alzr - acn*fzn/qn;
saam = bhd/vah;
gamo = arsin(saam);
thhn = gamo + alon*cos(fihn);
sthn = sin(thhn);
ctnh = cos(thhn);
csim = (bux + bzo*sthh)/(bxo*cthh);
ta = ( buz * buz + buy * buy ) * ( cthh * cthh);
tb = -2.*(bzo + bux*sthh)*buz*cthh;
tc = pow(bzo + bux * sthh,2) -pow(buy * cthh ,2);
dis = tb*tb - 4*ta*tc;
disr = sqrt(dis);
cfm1 = 0.5*(-tb + disr)/ta;
cfm2 = 0.5*(-tb - disr)/ta;
sfm1 = buy*(cfm1 * cfm1  - 1.)/(buz*cfm1 - bzo*cthh - bxo*sthh*csim);
sfm2 = buy*(cfm2*cfm2  - 1.)/(buz*cfm2 - bzo*cthh - bxo*sthh*csim);
fmpls = fim + chn*ot;
snmo = sin(fmpls);
dsf1 = abs(sfm1 - snmo);
dsf2 = abs(sfm2 - snmo);
if(dsf2 < dsf1) goto ten;
cfm = cfm1;
sfm = sfm1;
goto twnty;
ten: cfm = cfm2;
sfm = sfm2;
```

81

```
twnty: fim = arsin(sfm);
ssim = (sfm - buy*cfm/buz)*buz/bxo;
sim = arcos(csim);
if (ssim < 0) sim = tpi - sim;
if ((sim>tpot) && (sihn < pot)) sihn = sihn + tpi;
if ((sim<pot) && (sihn > tpot)) sihn = sihn - tpi;
rsi = sim - sihn;
rfi = fim - fihn;
ral = amn - alhn;
rh = hm + no - non;
sfih = sin(finn);
cfih = cos(tinn);
tthn = sthh/cthn;
c0 = rkbh*rn;
c1 = fxn*stnh - fyn*sfih*cthh - fzn*cfin*cthh - q
   + rk1*rh + onhn;
c2 = rk2*rh;
cbp = rkop*rfi;


c3 = pdn + rk3*rfi + ohpn;
c4 = rk4*rfi;
ccp = rkbq*ral;
c5 = odn + rk5*ral + ohqn;
c6 = rk6*ral + (fzn + q*cfih*cthh)/vah;
cdp = rkor*cfih*ctnn*rsi;
c7 = rdn + rk7*cfih*cthh*rsi + bhrn;
c8 = rk8*rsi;
bhhp = hhhn + c0*dt;
hhap = hnd + c1*dt + c0*att;
hhp = hhn + (hho + c2)*dt + c1*dtt + c0*dtq;
bhpp = bhpn + cor*dt;
phnp = phn + c3*dt + cbp*att;
finp = finn + (nhn + (qhn*sfih + rhn*cfih)*tthh + c4)*dt
   + (c3 + (c5*sfih + c7*cfin)*tthh)*dtt
   + (cbp + (cco*sfih + cdp*cfih)*tthh)*dtq;
bhjp = bnan + ccp*at;
qhnp = qhn + c5*jt + cco*dtt;
alhp = alnn + (crn + c6)*dt + c5*att + ccp*dtq;
bhrp = bhrn + cap*dt;
rhnp = rnn + c7*jt + cap*dtt;
sihp = sihn + c8*at + ((rhn*cfih + qhn*sfih)*dt
   + (c7*cfin + c5*sfih)*dtt)/cthh
   + (cdp*cfih + ccn*sfih)*dtq/cthh;
t = t + dt;
bhhn = ohhp;
hhn = hhap;
hhn = hnp;
bhpn = bhpp;
bhan = bhgp;
bhrn = onrp;
phn = phnp;
qhn = qhnp;
rhn = rhnp;
finn = finp;
alnn = alhp;
sihn = sihp;
goto read;                        82
```

REFERENCES

1. DeBra, D.B., and Bryson, A E.. Minimum Cost Autopilots
   for Light Aircraft. Sixth IFAC Symposium on Automatic
   Control in Space. Tsakhkadzor, Armenian S.S.R., U.S S.R,
   August 1974.

2. DeBra, D.B., et al.. On the Applicability of Integrated
   Circuit Technology to General Aviation Orientation Estima-
   tion   NASA CR-151952, December 1976   ·

3. Sorensen, J.A   Application of State Estimation Techniques
   for Development of Low-Cost Flight Control Systems, NASA
   TMX, September 1976

4. Wingrove, R.C · Accident Investigation--Analysis of Air-
   craft Motions from ATC Radar Recordings. NASA Aircraft
   Safety and Operating Problems Conference. Hampton, Vir-
   ginia, October 1976.

5. Wingrove, R.C   NASA Ames Research Center (Private Com-
   munication)   October 1976.

6 Denery, D.C. NASA Ames Research Center (Private Communi-
   cation)   January 1977.

7. Etkin, B. Dynamics of Flight. Wiley. New York, N.Y.,
   1959.

8. Higgins, W.T.   A Comparison of Complementary and Kalman
   Filtering. IEEE Transactions on Aerospace and Electronic
   Systems   May 1975, pp. 321-325.

9. Anon   Instrument Flying Handbook. AC 61-27B. U.S.
   Department of Transportation   1971.

10. Franklin, G.F., and Powell, J D.   Digital Control.
    Stanford University Course Notes. 1976. (to be published
    as textbook - 1978).

11. Bryson, A.E., and Ho, Y C.. Applied Optimal Control.
    Blaisdell   Waltham, Massachusetts, 1969

12. Breza, M.J., and Bryson, A.E.   Minimum Variance Steady
    State Filters with Eigenvalue Constraints. Stanford Uni-
    versity, Stanford, Calif , 1975.

13 Berkstresser, B.K., et al.. Cessna 402B Data Acquisition
   System, NASA TMX, August 1977.